**ADDIS ABABA UNIVERSITY**
**SCHOOL OF GRADUATE STUDIES**
**SCHOOL OF EARTH SCIENCE**

# GEOLOGICAL STRUCTURES AND TECTONIC EVOLUTION OF THE NEOPROTEROZOIC TERRAIN OF GUWILA AREA, TIGRAI, NORTHERN ETHIOPIA

**BY**
**DESTA DAWIT**

**A thesis submitted to School of Graduate Studies of Addis Ababa University, in partial fulfillment of the requirements for the degree of Master of Earth Science (Structural Geology)**

**May, 2014**

# ADDIS ABABA UNIVERSITY
# SCHOOL OF GRADUATE STUDIES
## SCHOOL OF EARTH SCIENCE

GEOLOGICAL STRUCTURES AND TECTONIC EVOLUTION OF THE NEOPROTEROZOIC TERRAIN OF GUWILA AREA, TIGRAI, NORTHERN ETHIOPIA

**BY**
**DESTA DAWIT**

**ADVISOR: MULUGETA ALENE (PhD)**

**A thesis submitted to School of Graduate Studies of Addis Ababa University, in partial fulfillment of the requirements for the degree of Master of Earth Science**
**(Structural Geology)**

**May, 2014**

**ADDIS ABABA UNIVERSITY**
**SCHOOL OF GRADUATE STUDIES**
**SCHOOL OF EARTH SCIENCE**

# GEOLOGICAL STRUCTURES AND TECTONIC EVOLUTION OF THE NEOPROTEROZOIC TERRAIN OF GUWILA AREA, TIGRAI, NORTHERN ETHIOPIA

**BY**
**DESTA DAWIT**

| **APPROVED BY EXAMINING BOARD** | **SIGNATURE** |
|---|---|
| Dr. Seifu Kebede<br>Department chairman and Graduate committee | ...……..... |
| Dr. Mulugeta Alene<br>Advisor | …… |
| _____<br>Examiner | ……... |
| _____<br>Examiner | .…… |

**May, 2014**

## ACKNOWLEDGEMENT

Foremost, I would like to express my sincere gratitude to my advisor Dr. Mulugeta Alene for the continuous support on my study and research, for his patience, motivation, enthusiasm, and immense knowledge. His guidance helped me in all the time of research and writing of this thesis. Besides my advisor, I would like to thank Dr. Seifu Kebede, head of Earth Science Department for allowing me to use a petrographic microscope in order to analysis the thinsection. My sincere thanks also goes to Ato. Woldesilasie, a thinsection expert, for his willingness in preparation of the thinsection. I thank the community of Senkata and Guwila for their hospitality and for being kind to me. They helped me a lot during my field work. I gratefully acknowledge the assistance of my friends in Mekelle University, Gosaye Brhanu and Mickaele Giday for giving information about the area and also for going field with me until I have got acquainted with the area. Last but not the least; I would like to thank my family: my parents Dawit Ekaso and Rebka Badacho for their unconditional support both emotionally and spiritually throughout my degree.

## TABLE OF CONTENTS

## LIST OF FIGURES

## ABSTRACT

Precambrian rocks out cropping in the Guwila area fall under two major groups, the metasedimentary and metavolcanic groups. The metasediments are part of the Tambien Group and the metavolcanic rocks are part of the Tsaliet Groups, both of which occur extensively in the region. Phyllites in the study area have a sedimentary origin and hence they can be grouped under the metasedimentary rocks along with other units such as slate, dolomite, and limestone. The metabasites and metavolcanic breccias, on the other hand, constitute the Tsaliet metavolcanics. The metasedimentary rocks are the predominant units in the Guwila area. The rock units generally trend in the NE and dip NW. However changes in the dipping direction of foliation is noticed in some of the areas and the structural analysis based on field observation and streoplot revealed the presence of locally developed antiforms and synforms on the central part of the study area. Similar to most of the Neoproterozoic units in the northern part of Ethiopia, the rocks in the Guwila area are metamorphosed under a low grade greenschist facies; some of the units still preserve the original texture at mesoscopic and microscopic scales such as primary bedding in the metasedimentary rocks. Relict plagioclase minerals being replaced by calcite and sericite and presence of muscovite, chlorite, and epidote all indicate low grade metamorphism. At least two phases of ductile deformation are observed on the area. North-south directed deformation which resulted in the formation of F1 tight to isoclinals folds with steeply plunging fold axis is regarded as the first phase deformation. It is also responsible for the development of the regional foliation. Second phase is related to a N-S trending nearly horizontal folds with larger interlimb angle and the formation of crenulation lineation and also crenulation cleavage.

# CHAPTER – I INTRODUCTION

## 1.1 BACK GROUND INFORMATION

Most of the geological investigations carried out on the Northern part of Ethiopia that left everlasting impression on the Geology of the area conducted after the 1960$^{th}$ though the basic foundation laid long before the 1960$^{th}$.

According to various researches conducted on the region, the Neoproterozic metamorphic rocks of the entire region which forms the southern part of Arabian-Nubian Shield is of a very low grade compared to the southern part of Ethiopia which constitutes the Northern Shield of the Mozambique belt (Levitte, 1970; Beyth, 1971; 1972; Kazmin et al 1978; Tefera et al, 1996; Tadesse, 1997; Asrat et al., 2001; Beyth et al., 2003) , except a few small out crops in the northern part of the escarpment area identified by Garland (1980). According to him, few outcrops of the high grade metamorphic rocks are exposed on this area, it can, however, be detected in air and space photographs as wide as 10kms and 50km long distinguished by its dark photo tone.

The low grade metamorphic rocks of the Northern Ethiopia, the Tigrai basement complex, are broadly classified as the Tsaliet and the Tambien group based on the origin, age, and types of rocks that each groups are attributed to (Beyth, 1972; Garland, 1980). Among the two groups, the Tsaliet goup is composed of rocks with volcanic origin that erupted during arc-accretion (~775-740Ma) (Miller et al., 2009) that latter metamorphosed in to a low grade metavolcanic rocks of various kinds including agglomarates, tuffs, mafic to felsic volcanic flows, and volcano-clasitic sedimentary rocks (Beyth, 1971; Tefera et al., 1996: Sifeta et al., 2005) which are lithostratigraphically beneath the Tambien group of sedimentary origin.

The Tambien group consists of slates, phyllites, greywakes, limestone, quartizic dolomites (Beyth et al., 2003) deposited on the geosynclinals basins of the region as opposed to the Tsaliet metavolcanics which are found on the anticlines. They are exposed on four isolated synclinoria, from west to east; Shiraro, Mai Kenetal, Chemit and

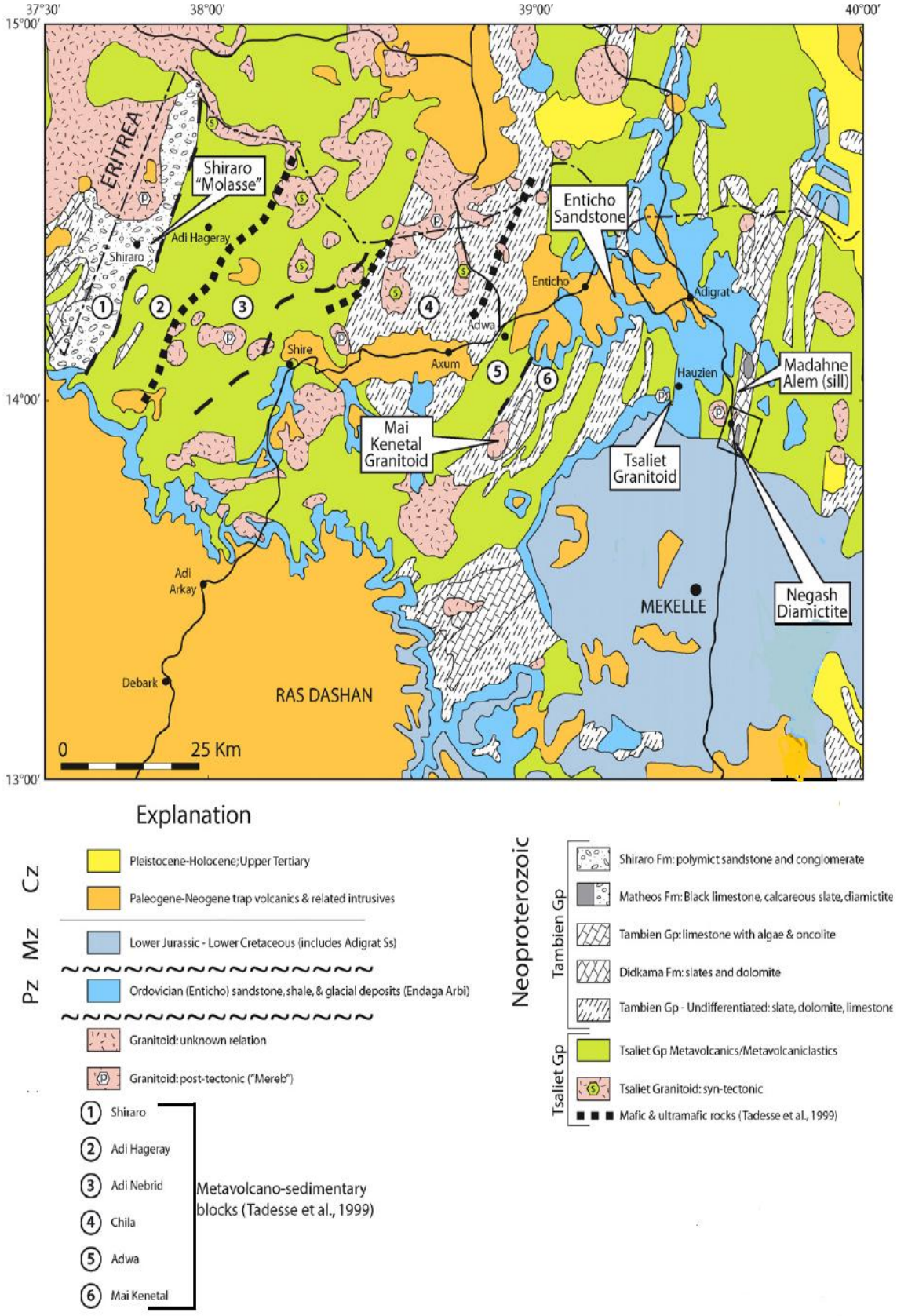
37°30'
38°00'
39°00'
40°00'
15°00'
14°00'
13°00'
ERITREA
Shiraro "Molasse"
Adi Hageray
Shiraro
Enticho Sandstone
Enticho
Adigrat
Adwa
Axum
Shire
Hauzien
Madahne Alem (sill)
Mai Kenetal Granitoid
Tsaliet Granitoid
Adi Arkay
MEKELLE
Negash Diamictite
Debark
RAS DASHAN
0
25 Km
Explanation
Cz
Pz Mz
Pleistocene-Holocene; Upper Tertiary
Paleogene-Neogene trap volcanics & related intrusives
Lower Jurassic - Lower Cretaceous (includes Adigrat Ss)
Ordovician (Enticho) sandstone, shale, & glacial deposits (Endaga Arbi)
Granitoid: unknown relation
Granitoid: post-tectonic ("Mereb")
1 Shiraro
2 Adi Hageray
3 Adi Nebrid
4 Chila
5 Adwa
6 Mai Kenetal
Metavolcano-sedimentary blocks (Tadesse et al., 1999)
Neoproterozoic
Tambien Gp
Shiraro Fm: polymict sandstone and conglomerate
Matheos Fm: Black limestone, calcareous slate, diamictite
Tambien Gp: limestone with algae & oncolite
Didkama Fm: slates and dolomite
Tambien Gp - Undifferentiated: slate, dolomite, limestone
Tsaliet Gp
Tsaliet Gp Metavolcanics/Metavolcaniclastics
Tsaliet Granitoid: syn-tectonic
Mafic & ultramafic rocks (Tadesse et al., 1999)

Figure 1.1 Distribution of rock types in Northern Ethiopia, Tigrai (Modified from Avigad et al., 2007)

Negash forming probably unconformable contact with the underlying older Tsaliet metavolcanics (Beyth, 1971, 1972; Miller et al., 2009).

The metasediments of the region are used to infer the paleo-climate of the region during its deposition. The sedimentary records of the Neoproterozoic age, for example, preserves abundant evidence of glaciations between *c.* 760 and 580Ma some with low latitude paleo-magnetic inclination, suggesting that several widespread icehouse fluctuations of Earth's climate state occurred prior to the first appearance of macroscopic heterotrophic life (Stern 1994; Miller et al., 2009)

The Tigrai basement complex in general is characterized by steeply dipping and extensively folded, low-grade metamorphic rocks intruded by various granitic and mafic intrusions (Taddese, 1997; Asrat et al., 2003). Intrusive igneous rocks of granitic origin collectively known as 'Mereb' Granites (Beyth, 1972) that post dated the tectonic activities in the area penetrates the older units of metamorphic rocks of both volcanic and sedimentary origin with almost circular massif consisting of monzogranites, granodiorites, diorites-gabrodiorites, and hybrid diorites (Asrat et al., 2003). The metamorphic rocks found near the granitoids commonly exhibit a poiklitic texture due to the heat released from the intrusive granitic bodies. Potential economic mineral deposits usually associated with these granitoids found in the northern Ethiopia because the post tectonic granitic intrusives facilitates the hydrothermal activities while the highly foliated Precambrian host rocks controlling the nature of mineralization (Tadesse et al., 2003).

## 1.2 LOCATION OF THE STUDY AREA

The study area, Guwila, is found in the Saesie Tsaedaemba district which is located in the eastern zone of Tigrai regional state. It is located 16km east of Senkata, the administrative center of the Saesie Tsaedaemba located at about 95km northeast of Mekelle town. The area is located between the geographic co-ordinates of: $14^{o}00'00"$ to $14^{o}03'53"$ and $39^{o}37'13"$ to $39^{o}39'43"$ at the southern border of 1430 D3 SINKATA (FIREWEYI) sheet.

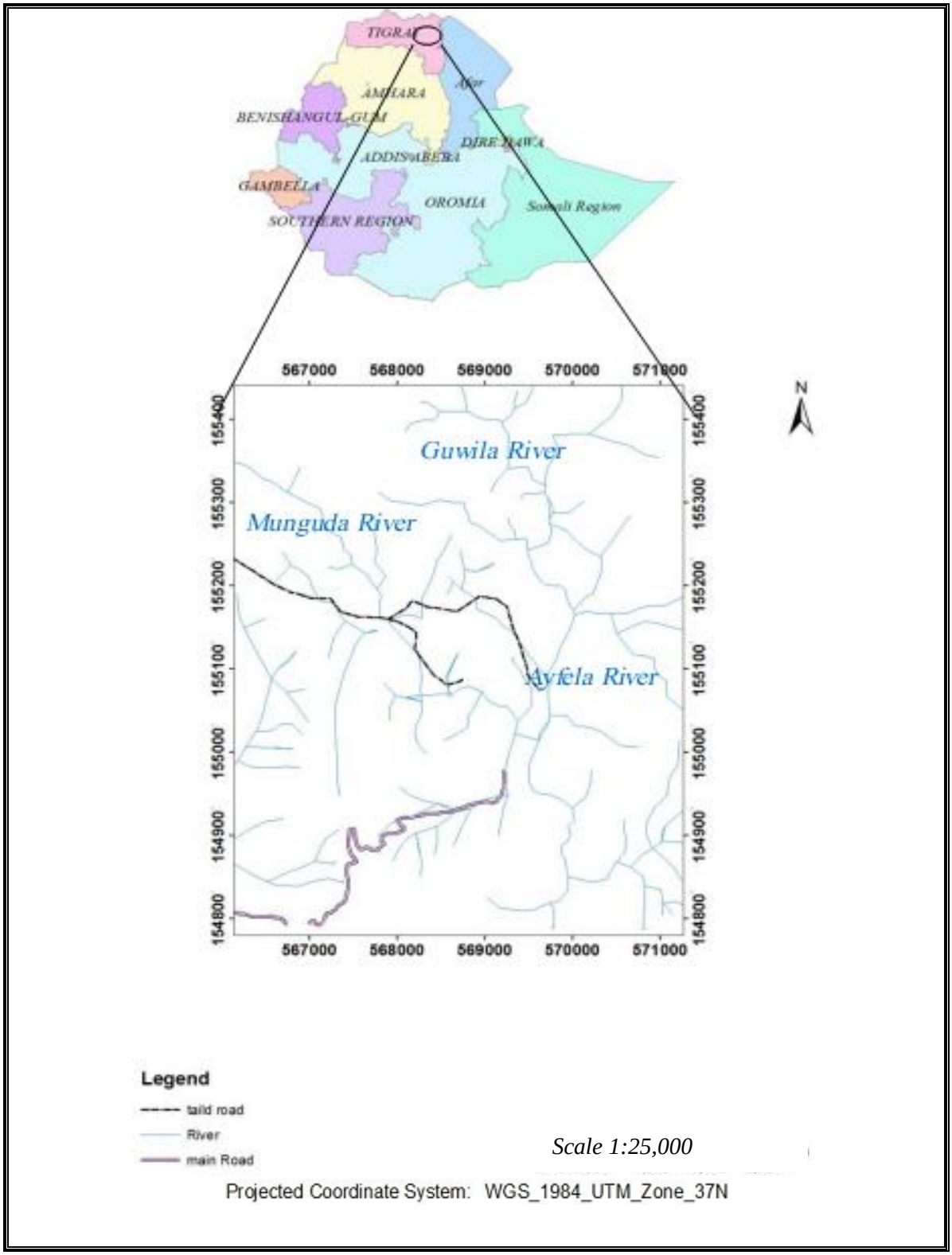


Figure 1.2 Location map of the study area

## 1.3 ACCESSIBILITY, CLIMATE AND PHYSIOGRAPHY OF THE STUDY AREA

Senkata town which was the base station for the field work is accessible through Mekelle Adigrat highway. The particular study area, Guwila, however is difficult to access with a transport Mini-Buses going only once a week though there is a gravel road from Senkata to the area. The shortest foot trails to the area through the highly rugged topography were followed to access the area.

The study area in general is characterized by a highly rugged and undulating landscapes represented mainly by large ridges, very steep to moderately steep slopes with lowlands and deep gorges having a fewer flat topographies formed by the alluvial deposits at and near the center of the basin. Minor dry bed streams with few perennial streams exists in the area dissecting the lowlands flowing generally from west to the basin in the east and some of them are used as the traversing line since they exposed the rock units.

The climatic condition of the study area is characterized as intermediate between hot arid and humid climate with mean annual temperature between $18^{o}$c and $27^{o}$c and mean annual rainfall between 410 and 820mm. The amount and distribution of rainfall is highly variable from season to season. Most of the annual rainfall is received during the summer especially in the two months of the year, July and August.

The vegetation cover of the study area is relatively poor. However there is lots of terracing is done on most of the hills of the area by the local people to increase the vegetation cover of the area and encouraging results have been obtained so far which are clearly seen on the area. The common types of trees observed are shrubs, grasses, thorn bushes and deciduous trees.

## 1.4 SIGNIFICANCE OF THE STUDY

Many researchers have spent a great deal of their time on the Northern Ethiopia and the Arabian-Nubian Shield in order to understand the tectonic evolution of the region and have tried to deduce some basic processes the area have undergone throughout the geologic history. The formation of major synformal and antiformal structures and the

constituent units of those folded structures provide much information about its evolution and major geological events occurred in the area since the Precambrian era.

The Negash syncline is one of the major synclinal structures in the region. Guwila is found in the northern part of the Negash syncline and the tectono-dynamics responsible for the formation of every structures and metamorphism in the Negash syncline also holds for the Guwila overturned syncline and other structures in the basin.

The area lacks detail investigation either to support or to doubt the already developed framework about the formation of the geosynclinal structures of the area. This research tries to look at the details of the major and minor geological structures in relation to the regional trend. Rock units and geological structures will be indicated on 1:25,000 scale geological map much larger than previous quarter million geological map by Garland (1972) of Adigrat area. Thus it will have a great contribution to the future studies on the area.

## 1.5 OBJECTIVE OF THE STUDY

### 1.5.1 GENERAL OBJECTIVE

The main objective of the study is to identify the major and minor geological structures and to analyze the deformations history of the Precambrian units in the Guwila area. Locating the existing geological structural features of the area formed as a result of regional tectonics showing how the area has been evolved throughout the geological time and to what kind of stress it was subjected to is what this thesis aimed to find out.

### 1.5.2 SPECIFIC OBJECTIVES

- Produce detailed map of the major and minor geological structures such as folds, faults, dykes, veins, etc
- Describe the lithology and Stratigraphy of the units in the area
- Determine the characteristics of the observed metamorphosed meta-volcanics and meta-sediments of the study area
- Determine the deformation phases by detailed structural and kinematic analysis of the suitable outcrops

- Understand the tectonic history of the area

## 1.6 METHODOLOGY

### 1.6.1 FIELD WORK

All the necessary procedures have been followed before the field work so as to understand what has to be done during the field work based on the objective the research to effectively collect the necessary inputs for the research. All available secondary data such as topographic map and geological map were collected and observation of the study area from aerial photo and satellite image analysis were done. Literature review to have a general framework of the geology of the area and delineating the study area from the topographic map were also conducted before the field work. Selection of suitable traverse line based on the accessibility and variety of the rock units which would be encountered along the traverse line and some of which are through the dry bed streams. Most of the selected traverse lines are directed from west to east based on the assumption that the different rock units are encountered through this line. Twenty five (25) oriented samples were collected for petrographic and micrstructural analysis during the 12 days of field work from which 11 samples selected for final thin section preparation.

The field studies in general include:

- Mapping of the various rock units and geological structures such as, faults, folds, foliation, lineation, dikes and veins at a scale of 1/25,000;
- Preparation of detailed sketch maps and cross-sections in order to describe the mesoscopic structures, boundary relationships, and lithological variations in defined rock units;
- Detailed structural/kinematic analysis of suitable outcrops to determine the number of deformational phases
- Measurement of attitude for foliation and associated mineral lineation.

### 1.6.2 POST-FIELD WORK

Transferring structural, foliation and other measurements on the field sketch map in to a net the same scale map from which a well developed geological map using Arc-GIS will

be produced and also compilation of all field data to get meaningful information out of it. Thin section is prepared in order to analyze the petrography and microstructure of the rocks representing each units as well as structural data analysis is done from field observation and measurements.

#### 1.6.2.1 LABORATORY ANALYSIS

Petrographic and micro-structural analysis of 11 representative thin sections from all units has been done. The orientation and nature of fabrics observed on the thin section is used to deduce its general character. The dominant mineral constituent of the rocks to give the appropriate naming of the rock types and study of the boundary relationship of the minerals from the thin sections to characterize its metamorphism in relation to the tectonic activity of the area is also carried out.

#### 1.6.2.2 STRUCTURAL DATA ANALYSIS

Analysis of data collected from the field using *Stereonet 8* (Rick Allmendinger, 2013) software to have a wider picture of the orientation of geological structures such as foliations, lineation, joints and the nature fold structures of the study area. Arc-GIS is also used to prepare the location map of the study area and to produce detailed geological map on which major structures and attitude of foliations including the lithologies are indicated.

## 1.7 PREVIOUS WORK

The scientific investigation of the geology of Ethiopia began in the 19$^{th}$ century. Unlike the other region, the northern parts of Ethiopia have got much of the researchers attention during this period of time. Garland (1980) in his book points out some of the pioneer researchers that explored the region, and their works. Ruppel in 1838 and Vignaud in 1843 tried to identify the rocks of this region. However, the most important contribution to the geology of Ethiopia, according to Garland (1980), came from the two staff officers of French army who classified the rocks into gneissic, phyllitic, mafic, oolitic, sedimentary and extrusive terrains in their works of 1844 and 1847. During the British expedition to Ethiopia in 1867-1868, the British Geologist W.T.Blanford made the scientific observations of some parts of the northern Ethiopia according to Tadesse

(1997) and Garland (1980). His stratigraphic sequence from youngest to oldest as cited in Garland (1980) is as follows;

1. Recent formations- soils of the highlands: coral islands of the red sea; alluvial deposits near the cost:
2. Aden series of the volcanic rocks bordering the Red sea:
3. Trappean Sereies (later simplified to Trap series:
   a) Magdala group (Upper, basalts with trachytes):
   b) Ashangi group (Lower, basalts):
4. Antalo limiestone:
5. Adigrat sandstone:
6. Metamorphic rocks.

Various studies have been conducted since then that gave us better understanding of the geology of Ethiopia which we use as a base map for the current geological investigations. Levitte, 1970; Beyth, 1971; Kazmin et al., 1978; Garland, 1980; Tefera et al., 1996; Tadesse et al., 1999; Asrat et al., 2001; Miller et al., 2009 are some of the researchers investigated the Northern Neoproterozoic basement sequences of Ethiopia in detail.

According to Beyth (1971), Kazmin (1973), and Kazmin et al., 1978 the basement complex of the northern Ethiopia is the youngest of the Precambrian rocks of Ethiopia and is classified as the upper complex. However, the oldest lower complex in some of the northern portion of the Escarpment can also be detected in air and space photographs (Garland 1980). The Precambrian geology of Adigrat is represented by both complexes. The lower complex according to Garland (1980) has limited development in this area which is built up by gneiss and the thick volcano-sedimentary units of the upper complex which is deposited in the geosynclinal basins. Asrat et al., 2001, argues that the Kazmin, 1978 classification of the basement rocks of Ethiopia based on age is not consistent with the existing geochronological, petrological and geochemical data. The evidences from theses data according to Asrat et al., 2001 shows that the lower complex which is part of the Mozambique Belt and the upper complex of the Arabian-Nubian Shield were built coevally with in the Pan-African Orogeny (950-500Ma).

Ethiopia is the place where the most intense collision between the Eastern and Western Gondwana occurred where the Arabian-Nubian Shield and Mozambique Belts meets, which is thus the transition between the low grade greenschist facies of the ANS and the high grade rocks of the MB (Avigad et al 2007). The general stratigraphy of the central part of Tigrai and its surrounding area is summarized as follow: a) the metamorphic and intrusive rocks of the Precambrian basement b) the Paleozoic-mesozoic sediments and tertiary trap volcanics c) the young sedimentary and volcanic rocks of the denakil depression (Levitte, 1970; Beyth, 1971).

Beyth (1971) also tried to classify the Precambrian basement complex as Tsaliet metavolcanics and Tambien metasediments. Tsaliet metavolcanics is the oldest of the two rock units which forms the base of the Tambien group outcrops in the anticlinoria while the youngest Tambien metasediments out crop in the synclinoria as examined by Beyth (1971). Sifetal et al., 2005 described the contact between these two major groups as ranging from seemingly conformable and gradational to fault bounded. These low grade deformed Neoproterozoic supra-crustal succession of the Tigrai area are sporadically preserved in fold and fault structures (Miller et al., 2009).

Tadesse (1997) argues that all the Precambrian metamorphic terrain of Ethiopia cannot be generally represented by a unified stratigraphic succession. He rather classified the stratigraphy of Axum area in terms of tectono-stratigraphic blocks and six blocks were identified which have a unique internal stratigraphy and structural details: the Mai kenetal block, the Adwa block, the chila block, the Adi Nebrid block, the Adi Hageray Block, and the Shiraro Block.

Tefera et al., 1996 highlighted the basement rocks of Ethiopia based on their chronological order: the archean complex, the early and the late Proterozoic rocks while preparing the geological map of Ethiopia at a scale of 1:2000, 000. Including the geological map of Ethiopia by Tefera et al., 1996, many other geoscientists have tried map to the geology of the region (eg. Arkin et al., 1971; Garland, 1972; Kazmin, 1972; Aguma and Kebede, 1976; Tadesse et al., 1996). These works have done a greater contribution to the understanding of the stratigraphy and tectonic history of the area.

Abdusalama and Stern, 1996 studied the structural style, ages and tectonic setting of the suture and shear zones of the Arabian Nubian Shield and divided them as two major events geochronologically as arc-arc sutures and arc-continent sutures as the first phase and post-accretionary structures as the second phase. Another researches Alene et al., 2006 considered the E-W shortening which is associated with the end phase collision between East and West Gondwana to be correlated with the post-accretionary structures. Alene et al., 2006 describes the tectonic history of the deformation belts of the Northern Ethiopia as the first phase of deformation D1 which is responsible for the formation of tight minor folds, elongation lineation and pervasive regional foliation, and the second phase of deformation D2 which formed due to the East-West shortening responsible for the formation of upright fold.

# CHAPTER TWO REGIONAL GEOLOGY

## 2.1 GENERAL REGIONAL GEOLOGIC SETTING

Geochronological data from different parts of the Pan-African high grade metamorphic rocks namely eastern and southern Africa, India, Madagascar, Sri Lanka, Arabia, and Antarctica, indicate that the assembly of Gondwana was a poly-phase processes with three main phases at ca. 760-730, 660-610 and 570-530Ma and from which the first two are attributed to the East-African Orogeny and the third event is the period of final assembly of Gondwana (Bingen et al., 2009). A relatively closer ages for theses phases are suggested by Abdusalam and Stern, 1996 (see Fig. 2.1) and Kroner and Stern, 2005. Condie (2003), states that about 50% of juvenile continental crust produced during this period is found in the Arabian-Nubian Shield and in other terrains that formed along the northern border of Amazon and West Africa. Arabian-Nubian Shield thus mainly comprises Neoproterozoic rocks formed, accreted, and deformed during the period from about 900-550Ma (Warden and Horkel, 1984; Stern, 1994; Abdusalam and Stern, 1996; Stern, 2002).

The Neoproterozooic Era encompases a proteracted orogenic cycle refered to as the 'Pan-African' Orogenic cycle (Stern, 1994). This forms crustal rocks of NE Africa and SW Arabia and consists of a series of volcano-sedimentary terrains which are dominantly low grade metamorphic rocks found in a number of NE-SW to N-S trending belts with minor moderate to high grade gneisses intercalation. (Tadesse, G. and Allien, A, 2005; Worku and Schandelmeier, 1996).

The collision of juvenile arc-terrains in ANS marks a critical aspect in the formation of end-Neoproterozoic supercontinent (Bailo et al., 2003). According to Stern (1994), the Arabian- Nubian Shield (ANS) consists of Precambrian rocks exposed on either side of the red sea in western Arabia and north east Africa and comprises a collage of Neoproterozoic terrains and older crust caught up as the suture between east and west Gondwana. These Shields makes up the northern half of the East African Orogen and stretches from the southern Israel and Jordan south as far as Ethiopia and Yemen, where the Arabian Nubian Shield transitions into the Mozambique Belt (Kroner and Stern,

2005).

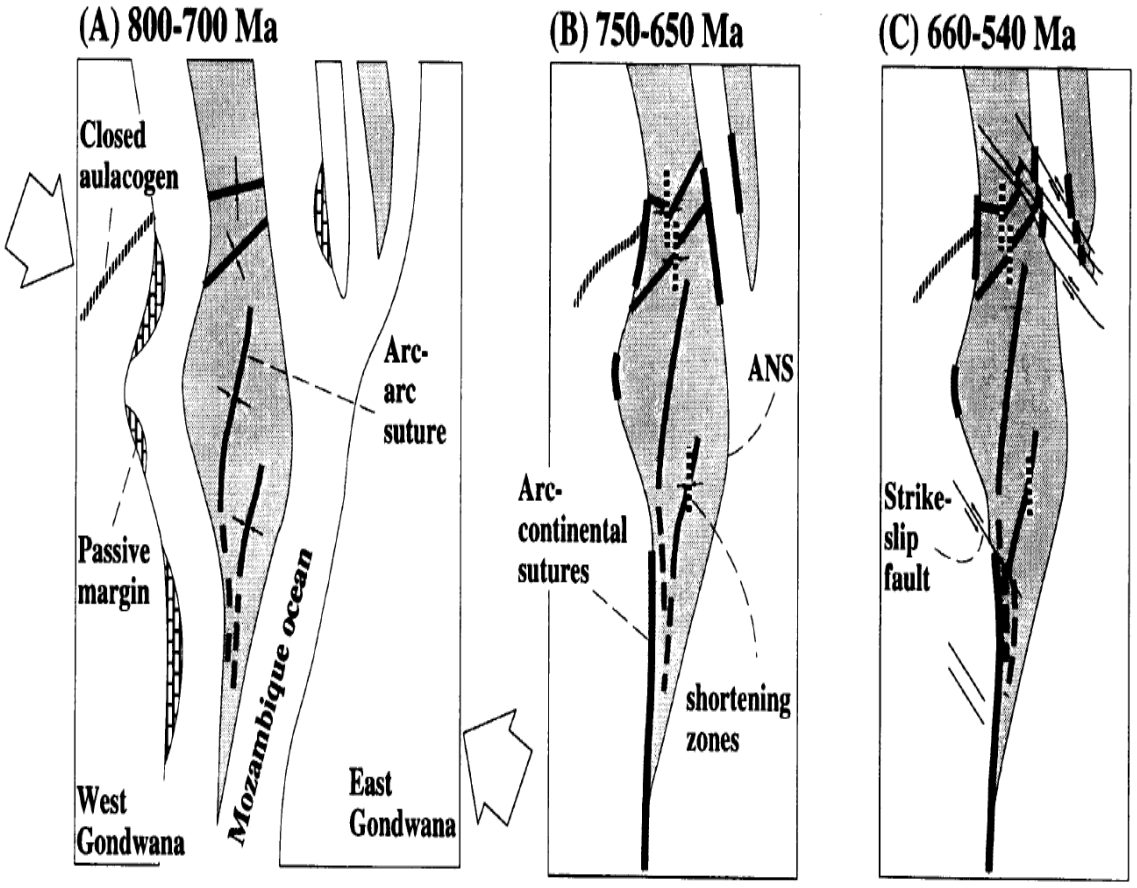


Figure 2.1 A sketch diagram illustrating the main phases of tectonic evolution in ANS; a) production of juvenile crust b) closing of Mozambique Ocean which formed EAO. c) Escape tectonics manifested by several strike slip faults (Abdusalam and Stern, 1996).

It took c. 300 Ma for the shield to grow starting at c. 870 Ma by the breaking up of Rodinia and the deposition of oceanic volcanic arcs on thin juvenile crust of the Mozambique Ocean, and terminated at c. 550 Ma by the transformation of the northern EAO into a passive marigin in the southern shore of Paleo-Teths (Johnson and Weldehaymanot, 2003).

The Mozambic Belt (MB) specially the North Eastern branch has a distinct geotectonic entity characterized by a predominantly ensialic structural setting and lengthy polycyclic evolution of which mainly the closing stage coincides with the Pan-African tectono-thermal episode (Warden and Horkel, 1984). The EAO origin is described by Stern, 2002, as the zones of greatest collisions on Earth.

The evolution of the East African Orogeny manifested a Wilson cycle with the following major tectonic, depositional and magmatic activities as discussed by Stern, 1994 and summarized by Beyth et al., 2003: (1) rifting of Rodinia followed by the creation of Mozambique Ocean, and formation of juvenile crust by sea-floor spreading (~850–750 Ma); (2) deposition of pelitic sediments on the eastern marigins of this ocean derived from sub aerial chemical weathering (~800 Ma); (3) subduction and continental collision of East and West Gondwana (750–634 Ma); (4) intrusion of late orogenic granitoids (~650 Ma); (5) transitional period in which escape tectonics occurred (~625–610 Ma); and (5) extensional tectonics and magmatic activities (~600–545).

Two major structures of Northeast Africa and Arabia which are the Arabian –Nubian Shield and the Mozambique Belt meet in Ethiopia (Kazmin et al., 1978). They described the following evolutionary history for the Precambrian basement rocks of Ethiopia: - i) Formation of ancient cratonic basement with high grade granulite facies metamorphism and tight isoclinal folding, perhaps of east-northeasterly or east-west direction and later the gneisses were subjected to high grade metamorphism of amphibolite facies ii) Accumulation of psammatic and pelitic sediments on the cratonic basement depressions iii) the rifting of ancient basement followed by opening of oceanic crust in the north which pinched out to the south continuing only as continental rifts along the whole or part of the Mozambique Belt iv) arc-type volcanism as a result of continental convergence and subduction of oceanic crust; and finally v) intrusion of post- kinematic plutons.

The basement rocks in Ethiopia covers significant portion of the country though much of these older rocks are covered by voluminous younger volcano sedimentary succession. Exposed rocks of the Precambrian era in some parts of the country suggest deep erosion

which removed the thicker volcano sedimentary cover. These rocks are exposed in different parts of the country mainly in the Northern, Western, and Southern parts of the country. It contains a wide variety of sedimentary, volcanic, and intrusive rocks-

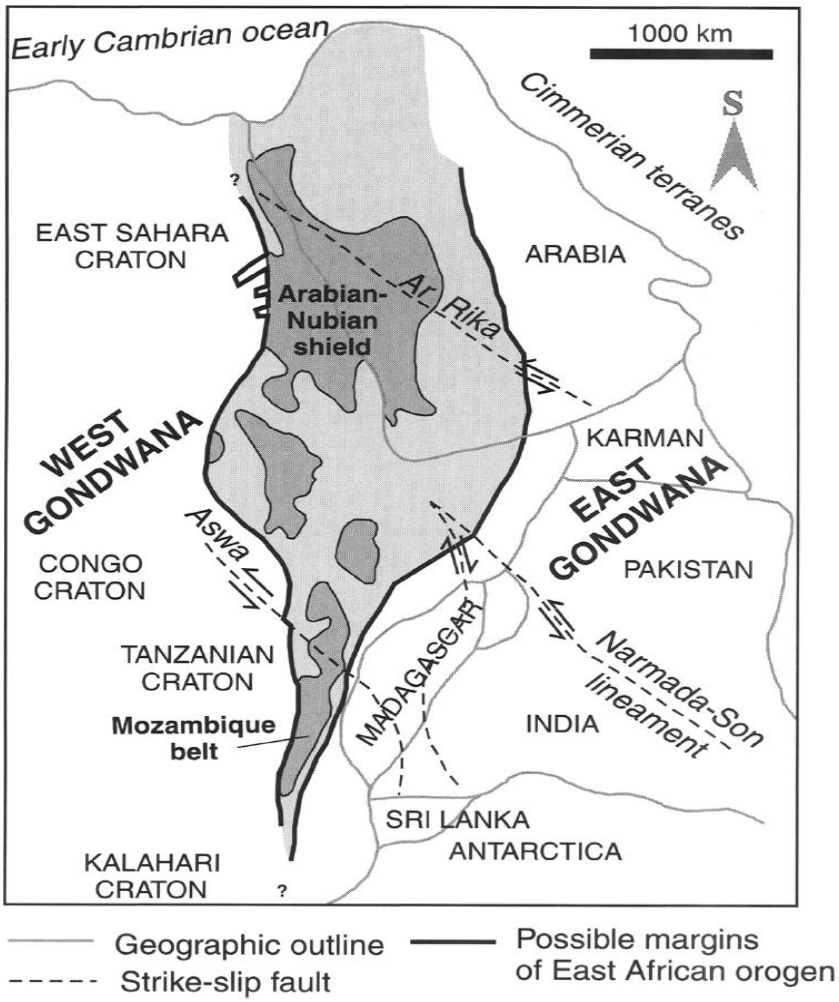


Fig. 2.2 Formation of East Africa Origin by collision of East and West Gondwana. It is bounded by major Sahara Metacraton to the west and possibly accreted microcontinents to the East (Stern, 1994 as cited in Johnson and Woldehaimanot, 2003)

which have been metamorphosed to varying degrees. In the Western part of Ethiopia, rocks of various types are exposed including high grade gneissic and migmatitic associations, and low grade meta-volcano sedimentary sequences intruded by syn- to post- kynamatic granodioritic and granitic plutons (Yihunie and Hailu, 2007). Warden

and Horkel, 1984 identified the Precambrian basement rocks in some parts of Eastern Ethiopia which can be correlated with the upper complex units of the Kazmin (1972) classification.

The Precambrian rocks of southern Ethiopia comprises high grade orthogneisses and deformed later metamorphosed granitoids, and ophiolitic fold and thrust belts composed of low grade volcano-sedimentary-ultramafic assemblages (Yibas et al., 2002). Worku and Schandelmeier, 1996, summarized the lithological and metamorphic conditions based on the distribution, deformation, and metamorphic evolutions of the rocks of the Adola belt in the southern Ethiopia as: a) gneisses and Schists of the Zembaba, Shakiso, and Sodda domains; b) mafic-ultramafic rocks and associated high grade metasediments of the Kenticha terrain; and c) low grade meta-volcanosedimentary sequences of the Megado terrain.

In general, the basement rocks found in the south and west, where granitic rocks and gneisses predominate, has been metamorphosed to higher grade than the Precambrian sequences in the north which is metamorphosed to lower grade greenschist facies (Mogessie et al., 2002).

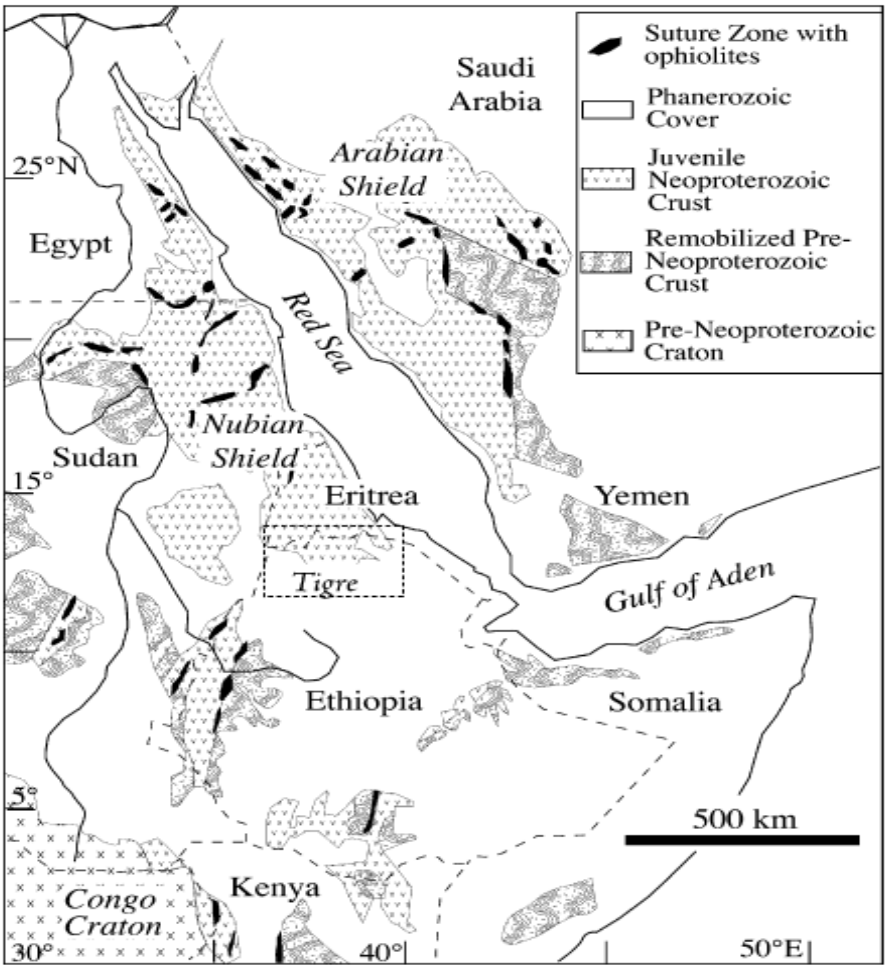


Fig. 2.3 The Neoproterozoic East African Orogen and the Arabian-Nubian Shield (Stern, 2002).

## 2.2 GEOLOGY OF TIGRAI BASEMENT COMPLEX

Levitte (1970), Beyth (1971) and Tadesse et al., 2003 classified the main rock types of Ethiopia as 1) the Precambrian lower and higher metamorphic rocks intruded by syn- to post-tectonic granitoids forming the Basement complex 2) the late Paleozoic to Mesozoic marine and continental sediments overlying the Basement complex 3) The Cenozoic basic and felsic volcanic rocks 4) The volcano-sedimentary and volcanoclastic rocks, associated with the Cenozoic volcanics, including Early Tertiary, Late Tertiary and Quaternary sediments.

In Ethiopia, Precambrian rocks outcrop in different parts of the region and are classified into three main complexes; the lower, middle and the upper complexes (Kazmin, 1973; Kazmin et al., 1978). The basement rocks of the northern Ethiopia are part of the upper/younger complex of the Precambrian rocks of Ethiopia (Kazmin et al., 1978).

These complexes in northern Ethiopia are composed of two main units; the lower Tsaliet meta-volcanics and the upper Tambien group (Beyth, 1971; 1972). Considerable part of the northern Ethiopia is underlain by more than 1500m thick low grade belt which is called 'Tsaliet metavolcanics' (Levitte, 1970; Beyth, 1971; Kazmin et al., 1978; Garland, 1980) after the Tsaliet River in the Tigrai region and is presumably younger than the low-grade belts of the southern and western Ethiopia according to Tefera et al., 1996. The Tsaliet meta-volcanics dominates most of the basement rocks of the Tigrai region and is composed of green to purple schist containing stringers of quartz, epidote and calcite inter-bedded with white, black, green and pink quartzite; pink to light green gneiss and minor black limestone and light green marble (Beyth, 1971), generally ranging in composition from basalts to dacites, rhyolites and associated metasediments (Tefera et al., 1996). Accordingly the Tambien group, which is meta-sediment is distributed around four major inliers; Mai kenetal, Tsedia, Chemit, and Negash synclinorium (Beyth, 1971; Tadesse, 1999; Miller et al., 2003; Alene et al., 2006; Miller et al., 2009; Miller et al., 2011). The Metasediments bear evidences of shallow water origin such as ripple marks, crossbedding and mud cracks (Tefera et al., 1996).

Negash synclinorium is an elongated grabben running northwards from the Wukro fault belt to the north of Gunda gundie. The core of recumbent anticline east of Senkata is composed of graywake and this recumbent anticline is among the three main en echelon structures (two anticlines and one syncline) which define the Negash graben (Beyth, 1971). Garland (1980) described the Guwila river basin as a composite structure in the werii slate, didikama formation and limestone. Werii slate is fissile and preserve original sedimentary bedding and their X-ray diffraction analysis show the presence of quartz, chlorite and mica as major mineral. Calcite and plagioclase (albite) as minor constituents where as K-feldspar, magnetite, and kaoline as trace minerals (Sifeta et al., 2005). In the south it is bounded by faults on both sides and is topographically a depression of four

kilometers wide. Its western boundary with meta-volcanics is a series of faults and low angle thrusts; east of this boundary is a westerly recumbent anticline with an axis at $015^0$ having a core of greywacke/werii slate/ (Garland 1980).

Genna et al., 2002, notes the widespread extension, after the pan-African tectonism (690-590Ma), that brought about crustal thinning generated bimodal magmatism and significant dike swarms. This crustal thinning and low angle faulting caused rapid crustal exhumation and extensive erosion (Beyth et al., 2003). They also suggest the presence of the coupling of compressional and extensional structures in Ethiopia in the Mai Kenetal and Negash folds from their intrusions and quartz veining.

## 2.3 STRATIGRAPHIC AND STRUCTURAL FRAMEWORK OF THE TIGRAI BASEMENT COMPLEX

A comprehensive Neoproterozoic stratigraphy of the Tigrai area, Northern Ethiopia is given by Beyth (1971, 1972). Primary sedimentary structures such as graded bedding exists in this area indicating that the sedimentary sequence was laid down in a submarine environment with intense deformation making it difficult to recognize the younging direction (Tefera et al., 1996; Tadesse et al., 1999; Miller et al., 2009). Though the tightly folded and faulted characteristics of the Neoproterozoic rocks of the region makes it difficult to decipher the internal stratigraphy of the Tambien group, there are few way-up indicators showing fining upward sequences and phototropic organosedimentary structures showing the up- direction of sedimentation (Miller et al., 2009). The Tambien meta-sediments are younger in age than the Tsaliet meta-volcanics although there is an ongoing debate that they are deposited at the same time during the formation of arc-acretion arguing that volcanism and the deposition of the sediments from the continental area occurred simultaneously referring to the 'gradational contact' (Alene, 1998 as cited in Alene et al., 2006) between them and the age constraints though Beyth (1971) identified unconformable basal contact between them. Seemingly conformable and gradational to fault bounded contact is described by Sifeta et al., 2005. However they are generally believed to have occurred over an Iceland arc accretion complex during or after

the waning phases of arc magmatism and ended prior to the formation of East African Orogen (Avigad et al., 2007; Miller et al., 2009).

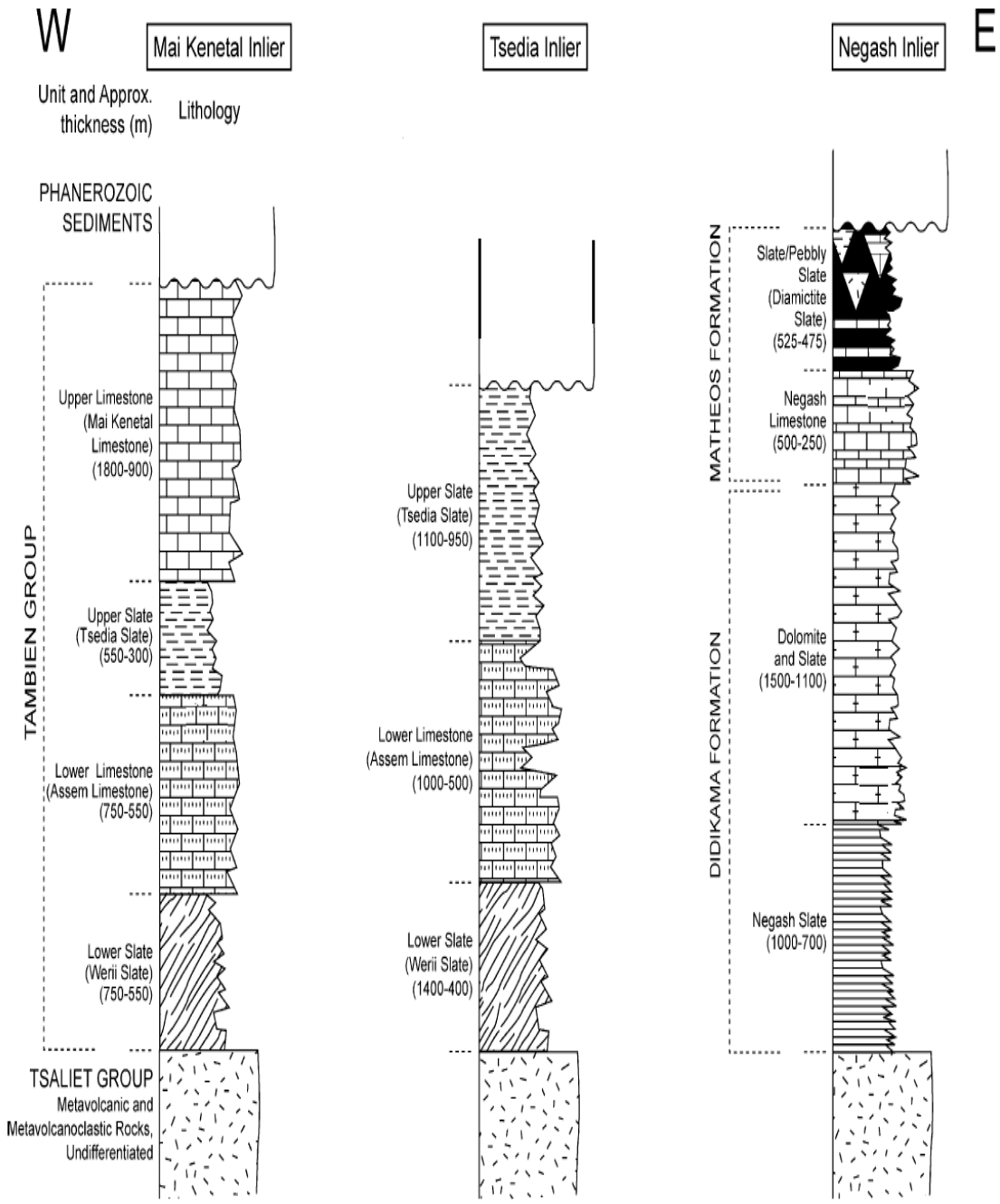

Figure 2.4 A diagram showing the general stratigraphic section of the metasediments underlying by the Tsaliet metavolcanics in the Mai kenetal, Tsedia and Negash synclines (Modified from Alene et al., 2006).

Four major formations were identified with in the Tambien group based on the Mai Kenetal type section and they are Werii Slate, Assem Limestone, Tsedia Slate, and Mai Kenetal Limestone from bottom to top respectively (Beyth, 1971; Alene et al., 2006; Miller et al., 2009). Garland(1980) subdivided the Negash Tambien group succession into the lower Didikama formation and overlying Matheos formation which are in turn divided in to four sub-formations a bit different from that of the Mai Kenetal, and it includes from bottom to top: Negash Slate, Dolomite and Slate, Negash Limestone, and Pebbly Slate (Alene et al., 2006). Tsaliet group is found in between or surrounding this synclinal structures at the eastern and western boundaries of them as an anticlinorium like the Tsaee and Bereh anticlinorium (Beyth, 1971). The stratigraphy of the Tsaee anticlinorium from bottom to top include: Dolerite intrusion, Andesitic aggrlomerate tuffs and lapilli tuffs with thin quartizitic beds, Andesitic tuffs, Black and pink quartzite and redeposited rhyolitic tuffs, and that of the Bereh anticlinorium represented two main rock sequences; the eastern one composed of phyllites interbedded with pyroclastic rocks and the western one composed of acidic volcanic rocks interbedded with intermediate and subordinate phyllites (Beyth, 1971).

The Neoproterozoic rocks of the Northern Ethiopia are preserved in the fold and fault structures and they are deformed into generally NNE trending folds and faults (Miller et al., 2009). The low grade volcanic and volcano-sedimentary sequences of the western Tigrai are affected by various shear zones particularly NE-SW trending mainly sinistral strike slip faults and thrusts verging either to the NW or SE (Tadesse, 1996; Tadesse, 1997; Tadesse et al., 1999).

Field relationships conducted by Tadesse (1996) of the linear and planar structures developed on the Zager mafic and ultramafic belt of the region shows the presence of simple shear structures. He also noted the presence of intrafolial folds formed by the transposed metamorphic layering, S-C fabric and other asymmetrically rotated objects indicating consistent oblique Sinistral shearing as a major deformational feature.

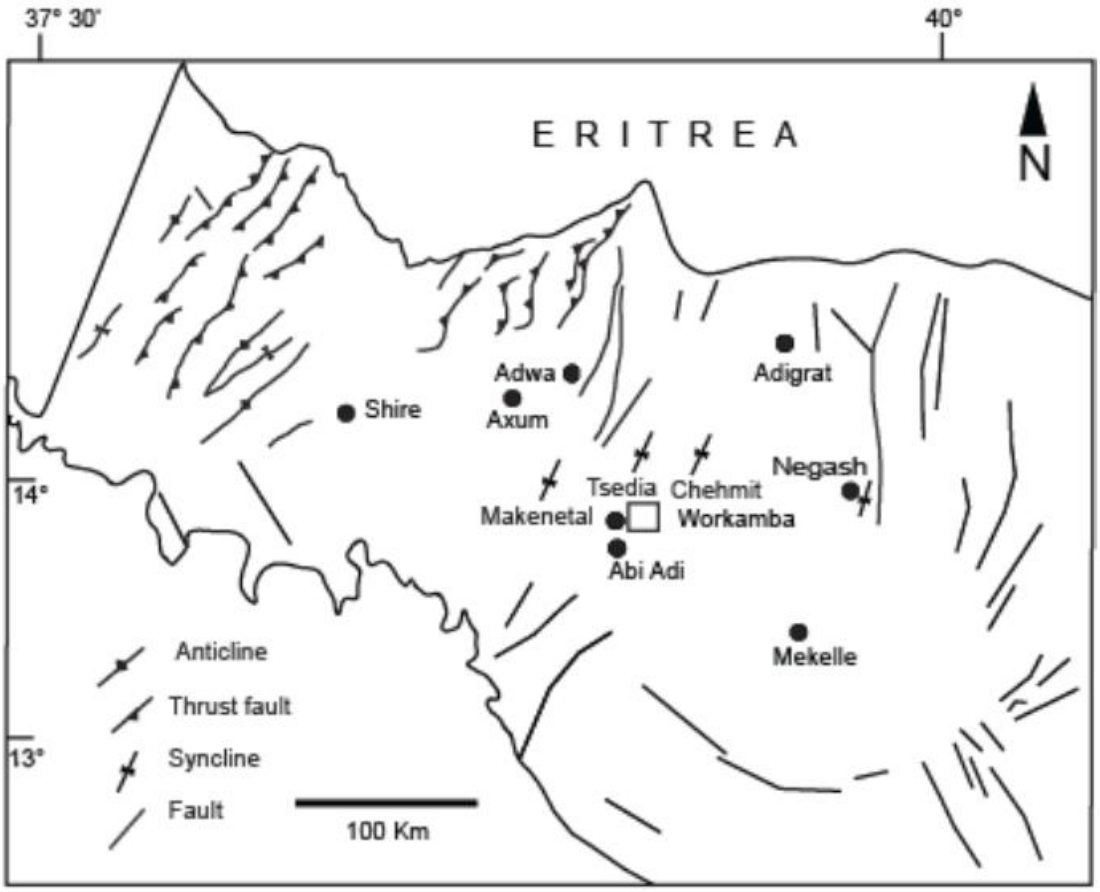


Figure 2.5 Distribution of major geological structures in Tigray area (Gebremariam, 2009)

Based on the principles of superimposition and crosscutting relation, Tadesse (1997), tried to identify about five phases of deformation on the tectonostratigraphic blocks of the Axum area. Each phase of deformation could be associated with different foliation, fold and lineation according to him. However, pervasive regional foliation trending NNW/SSE-NNE/SSW generally dipping to the west, and brittle structures which cuts earlier structures are attributed to the first and last phases of deformation respectively according to the structural analysis made by Tadesse (1997).

The two major units of the Precambrian metamorphic rocks of the Tigrai basement complex namely the Tsaliet metavolcanics and the Tambien metasediments are subjected to two major phases of folding D1 and D2 (Alene et al., 2006). D1 is caused by N-S

directed compression resulted local repetition of stratigraphy and the formation of tight minor folds with a wavelength of several mm to dm, elongation lineation and pervasive regional foliation and D2 is resulted from E-W shortening at the end stage of the collision between East and West Gondwana to yield long wavelength (about 8km), upright, open parallel folds without a significant cleavage, and thrusting (Alene et al., 2006). The E-W directed shortening deformation culminated with the development of northwest trending strike-slip faults and shear zones (Abdusalam and Stern, 1996). Major geosynclinals structures of the central Tigrai such as Mai Kenetal, Tsedia, Chemit, and Negash (Levitte, 1970; Beyth, 1971; Garland, 1980, Miller et al., 2003) which folded the younger Tambien group metasediment is formed by second phase D2 deformation (Alene et at., 2006). From the typical wavelengths of those folds, Miller et al., 2009 estimated the crustal shortening on the order of 200%.

Negash synclinorium is bounded to the east by normal faults of the Atsbi Horst and to the west by thrust faults at the boundary between the metavolcanics and metasedimets (Beyth et al., 2003; Miler et al., 2009). Before that, however, it is noted that Garland (1972) when mapping Adigrat area, indicated the presence of east dipping normal faults with some smaller thrusts at the western boundary of the Tambien metasediments with metavolcanics and reverse faults at the eastern boundary of the synclinorium with the metavolcanics in the Northern part of Negash syncline.

# CHAPTER THREE LOCAL GEOLOGY

## 3.1 INTRODUCTION

This chapter aims at describing the various lithologic units cropping out in the study area and their petrographic analysis in order to understand the metamorphic conditions and tectonic activities which affected the units in addition to the field observation.

The area is dominantly covered by metasedimentary rocks having a very rugged topography with few flat areas covered by a very recent alluvial deposit at the eastern part of the study area. The units are cut by generally east west running streams which exposed the rocks and structures. Metavolcanic rocks occupy the western part of the area bounding the Phanerozoic formations. The Precambrian rocks of the metavolcanic and metasedimentary units are covered by the Phanerozoic sandstone on some parts of the area. The rocks are metamorphosed to a low grade greenschist facies with some of them showing relict primary textures such as primary bedding and also relict primary minerals when observed under microscope. The primary textures are used to infer the protolith of the rocks and their degree of metamorphism.

The rocks were subjected to different phases of deformation which are responsible for the development of metamorphic fabrics such as foliations and lineations of various generations observed on the rocks both at mesoscopic and microscopic scale. Some of the rocks are strongly foliated especially slates and phyllites. They are crosscut by joints with no systematic sets and faults. The units found in the area in general from west to east include: metabasites, slates, metavolcanic breccias, phyllite, dolomite and slate intercalation, and meta-limestone.

The latter Phanerozoic sandstone occupies the eastern most part of the study area and also some of the southern parts overlying the Precambrian rocks. Among these units slate and dolomites intercalated with slate covers larger area relative to other units. Their orientation varies from NW to NE having an average dipping angle of about $60^0$ either to the west or to the east.

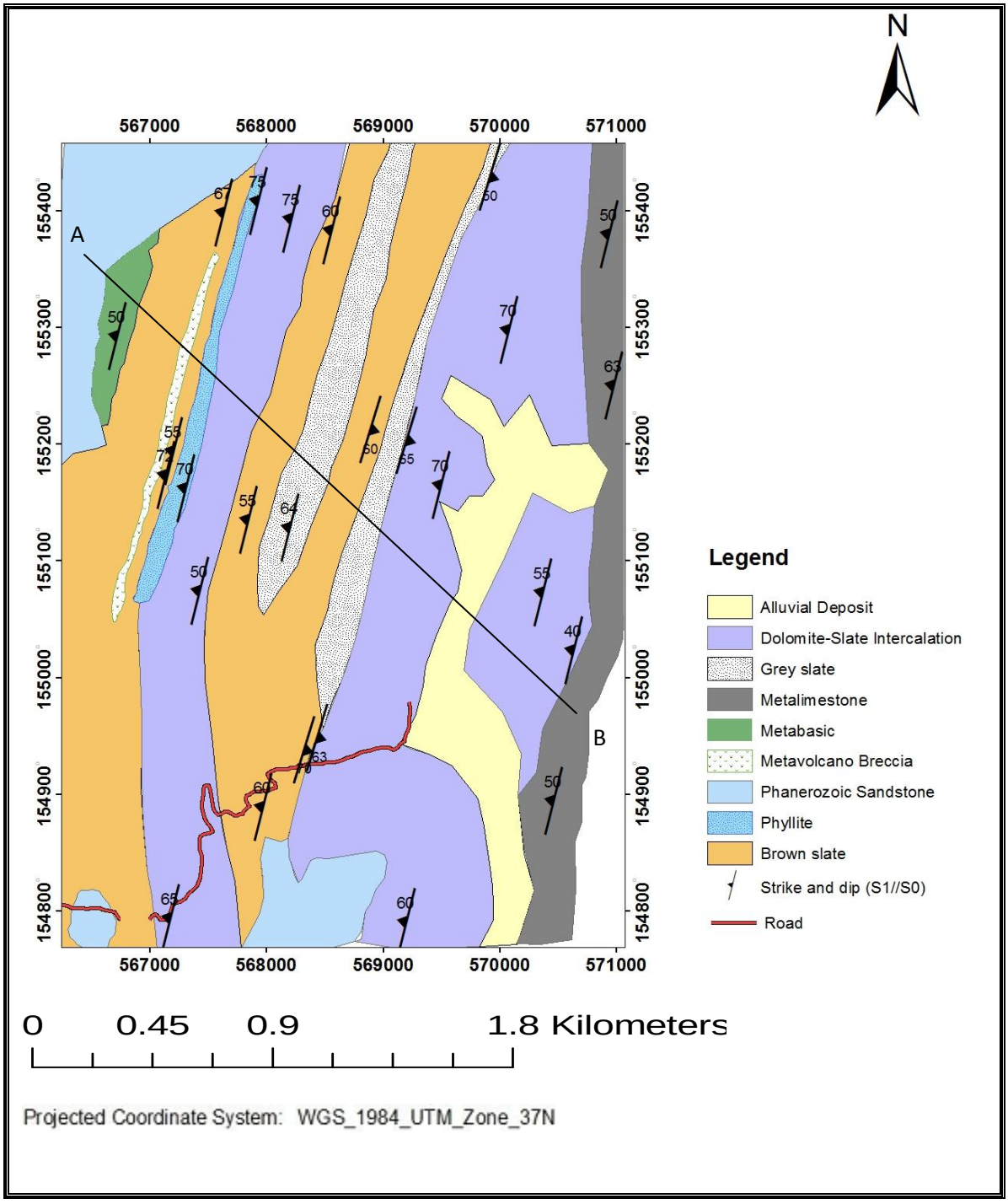
N
567000
568000
569000
570000
571000
155400
155300
155200
155100
155000
154900
154800
A
B
Legend
Alluvial Deposit
Dolomite-Slate Intercalation
Grey slate
Metalimestone
Metabasic
Metavolcano Breccia
Phanerozoic Sandstone
Phyllite
Brown slate
Strike and dip (S1//S0)
Road
0 0.45 0.9 1.8 Kilometers
Projected Coordinate System: WGS_1984_UTM_Zone_37N

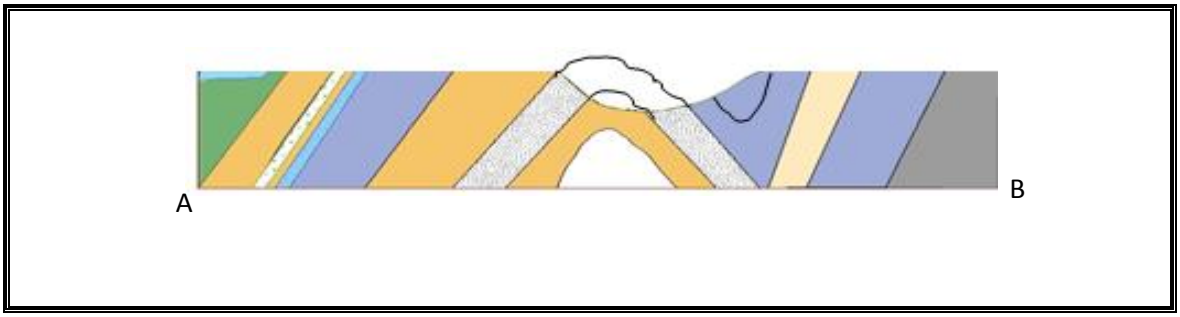


Figure 3.1 Lithological map and cross section of the study area

### 3.2 SLATE

It is very fine grained having different kinds of color including green, grey, brown with brownish and grayish dominating the slates in the area and they have strong parallel foliation forming the prominent regional foliation which generally trends in the NE to NW direction dipping either to the east or to the west at high angle. Measured foliation data indicates that the dominant dipping direction is to the west. Along the cleavage line they split into very thin layers on fresh unweathered slates but it is difficult on weathered slate because they usually form thick beds. The removals of secondary minerals such as pyrites giving it mottled appearance when the grain is finer and open spaces having the shape of pyrite grain when it is coarser. It forms gentle to very steep topography forming the highest cliff of the area having an altitude of about 2640m to the west of Guwila Abenea School. The unit has a thickness of more than 1km. Near Alegnta Kirkos church the lithologic unit of darker grayish unit is found sandwiched in between the slates. The upper slate in the western part of the study area is overlain by the latter coming Phanerozoic sandstone.

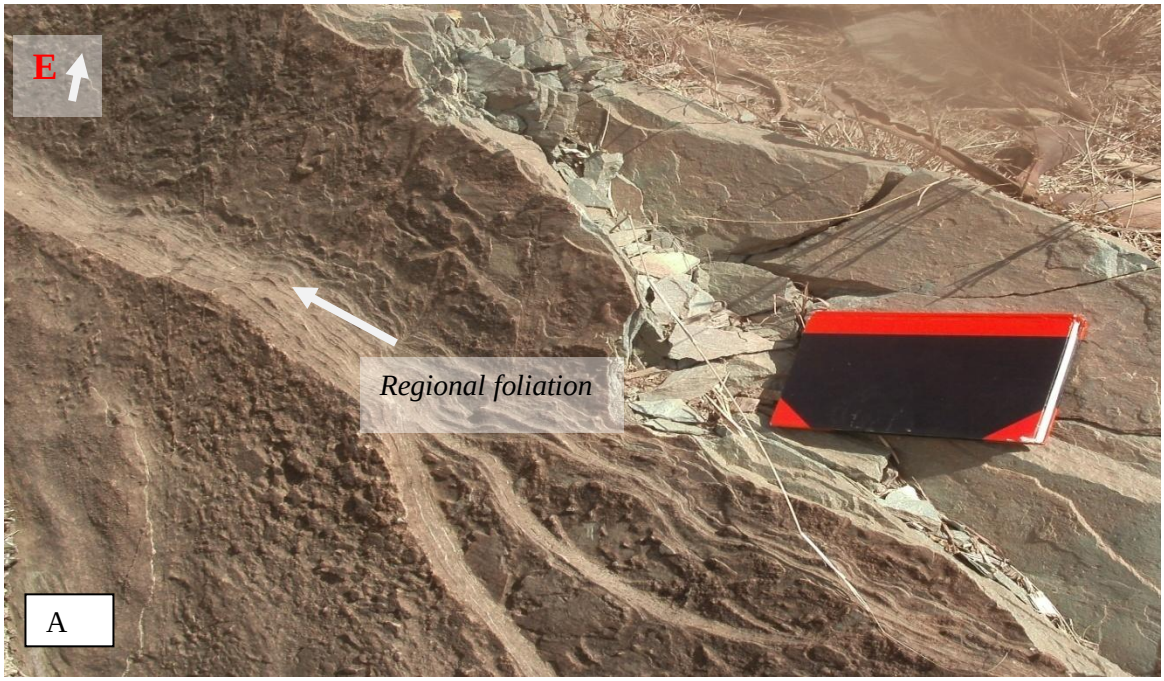



Figure 3.2 Slates from the study area A) Greenish slate showing prominent regional foliation orientated at N10W/65SW. B) Brownish slate cut by shallowly plunging joints. Orientation of the slate: N10E/75SE (Location; A: 0567522E, 1552265N; B: 0568888E, 1551958N). Picture taken while facing east.

### 3.2.1 PETROGRAPHY

Later quartz and calcite crystals are usually seen precipitated on the already formed pre-kinematic open spaces /GW6/. The foliation is defined by sericite micas and fine grained elongated quartz crystals which are deformed during the early period of deformation. Thin zigzag veins of quartz crosscuts the S1 pervasive foliation indicating that it is younger than the other quartz minerals which are aligned parallel with foliation /GW6/. Opaque minerals are found stretched linearly along fractures forming lines of opaque minerals /GW7/. Euhedral to subhedral opaque grains (pyrites?) are overprinted the foliation and they are randomly oriented (Fig 3.3 A). Thus they are post tectonic unlike other opaques. Solution surfaces which are parallel with each other and perpendicular (see Fig 3.3B) with the regional foliation are found formed by precipitation of insoluble minerals like clay minerals and iron oxides which appear dark both under PPL and XPL /GW6/ (Fig. 3.3 B). Chemical compaction dissolved the sutured grain boundaries of crystals leaving open spaces latter filled by this insoluble minerals. The rock is composed of 45% sericite, 35% quartz, 6% chlorite 4% plagioclase and about 10% of opaque minerals. Hence it is named as plagioclase-chlorite-quartz-sericite slate. Another rock represented by thin section /GW7/ contains: 35% sericite, 30%, quartz, 10% muscovite, 5% chlorite, 5% plagioclase, 15% opaque. And it is named as plagioclase-chlorite-muscovite-quartz-sericite slate. Pre- to syn- tectonic quartz crystals commonly exhibiting undulose extinction indicating that it was subjected to deformation that formed S1 foliation which is faintly crenulated by D2 nearly perpendicular to the earlier D1 deformation /GW7/.

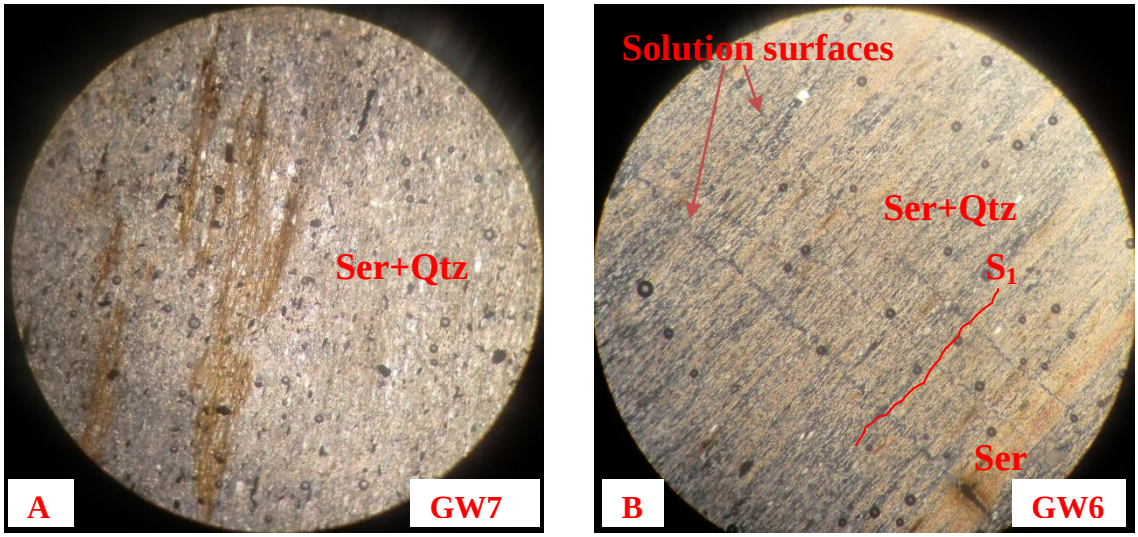


Figure 3.3 Microscopic photo-pictures of slates under cross polarization. A) Fine grained quartz and sericite. Post-tectonic opaque minerals overprinted the earlier sericite, and quartz minerals. B) Solutions surfaces across S1 foliation. Location of samples; A: 0567301E, 1551780N; B: 0568063E, 1554265N. (*Total magnification; 10x10=100x*).

### 3.3 METABASITE

This rock is exposed on the north western region of the study area bounding the sandstone unit unconformably overlain by them going farther west from the area. It has a greenish color because of the presence of the commonly greenish minerals such as chlorite and epidote. It has an average thickness of about 250m. This unit mainly forms a relatively gentle topography and is cut by seasonal river streams across its strike. The rock is less weathered compared to other rocks of the study area. The contact between the metabasites and adjacent slate rock is of a sharp type contact.

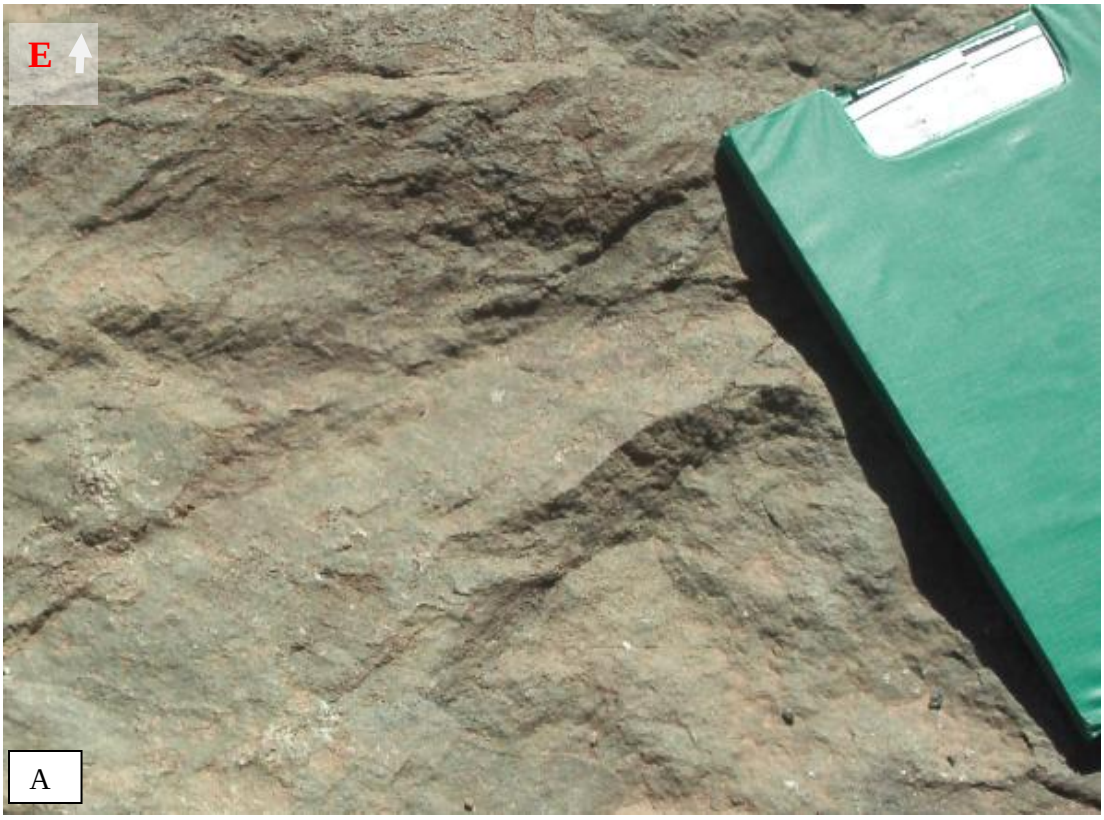
E
A


E
etrex
SUMMIT
GARMIN
B

Figure 3.4 Field photos of metabasic rocks. Location; A: 0566563E, 1550787N; B: 0566892E, 1553359N. Picture taken while facing west and east respectively.

### 3.3.1 PETROGRAPHY

It is composed of epidote, chlorite, quart, and plagioclase minerals. Polysynthetic quartz and other plagioclase minerals exist concentrated along some region. Calcite and chlorite crystals are also found through the boundaries of quartz grains. Quartz and epidote veins are observed in this sample. The rock is dominated by epidote minerals. The chlorites in between the quartz grow larger relative to the chlorites found along the boundaries. Quartz grain shows evidence of deformation implying that it was formed predating the deformation (Fig. 3.5A). The mineralogical composition of the rock is: 34% epidote, 27% plagioclase, 18% quartz, 15% chlorite, and 6% calcite. Therefore the rock is called calcite-chlorite-plagioclase-quartz-epidote metabasite.

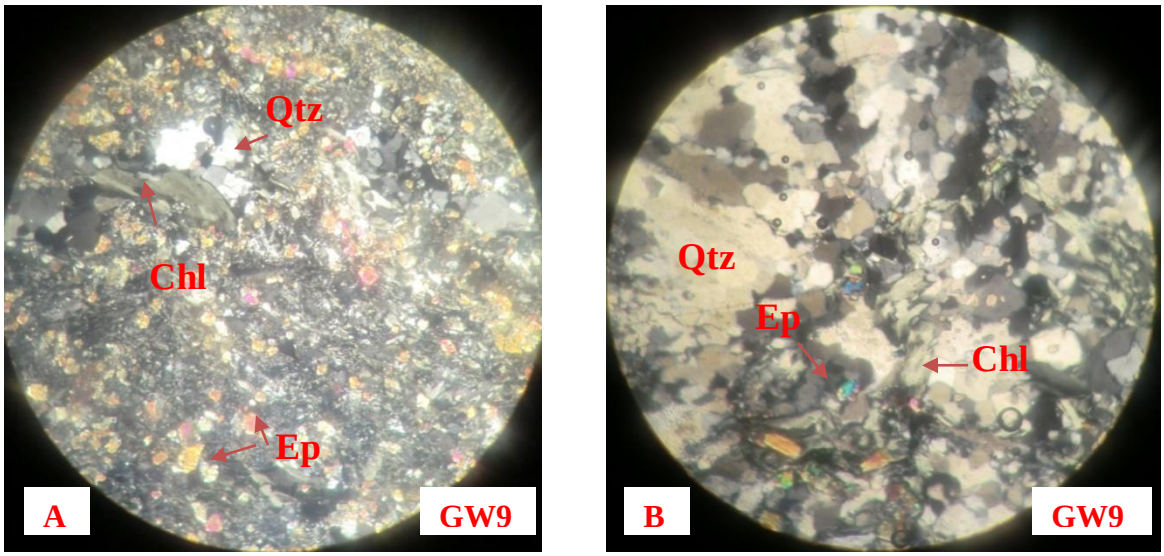


Figure 3.5 Photomicrographs showing various minerals in the metabasic rocks (observed under XPL). A) Quartz crystals showing undulatory extinction suggesting that it has experienced intracrystaline deformation B) Concentration of quartz minerals at certain region. Quartz crystals exhibit irregular boundaries. Sample Location; 0566892E, 1553359N. *Total magnification; 10x10=100x.*

### 3.4 META-VOLCANIC BRECCIA

The rock has a pale green color. The unit is found in between the slate bounded by them both to the west and to the east. It forms a very thin layer with a thickness of about 50m. The eastern part of this unit forms a very steep topography. The rocks is brecciated with clasts of varies type from dominantly quartz rich to mica reach clasts. Mica reach clasts are shinny with its characteristic foliation. The larger mica reach crystals are developed into a phyllitic grade with glittering mica crystals. The porphyroclast in this meta volcanic breccias are larger and clasts of about 30cm are measured on the field (Figure 3.6B).


Figure 3.6 Field photographs showing metavolcanic breccias from different areas. A) The clasts are deformed having ellipsoidal shape B) A clast of about 30cm on the metavolcanic breccias. Location; A: 0567134E, 1551897N; B: 0567114E, 1551843N. Direction of view is to the east.

Two kinds of lineation oriented in different directions are measured from this zone. The first is stretching pebbles with a general orientation of ENE-WSW (Fig 4.4A&B) and the second one is crenulation lineation generally oriented North-South (Fig 4.7A&B). The rock is also found on the southern regions of the study area at unmappable scale as minor lensoids of massive rocks.

### 3.4.1 PETROGRAPHY

It is highly brecciated with most of the primary plagioclases are being variably replaced by latter minerals such as calcite and quartz having finer inclusions of minor opaque minerals and also some of the larger laths of quartz and plagioclase are mechanically bended (Fig. 3.7B). Calcites are seen replacing plagioclases and they are both being replaced by quartz /GW10/. Well developed larger orthorhombic calcite crystals are precipitated between the open spaces. Dissolution of materials is commonly seen around

the grain boundaries of coarser plagioclase usually between two adjacent plagioclase grains. Euhedral to subhedral quartz minerals have sutured boundaries along their grains. Muscovite micas show ductile deformation /GW11/ forming asymmetric crenulation and the relatively resistant pre-tectonic quartz minerals affected the sequence of crenulation /GW11/. Calcites are often concentrated on certain areas. Larger polygozed crystals of quartz and subgrains with a wavy extinctions have a sutured boundaries probably formed by grain boundary migration /GW11/. They are generally pre- to syn-tectonic. Pre-kynematic plagioclases on some parts of the thin section are rimmed by quartz.

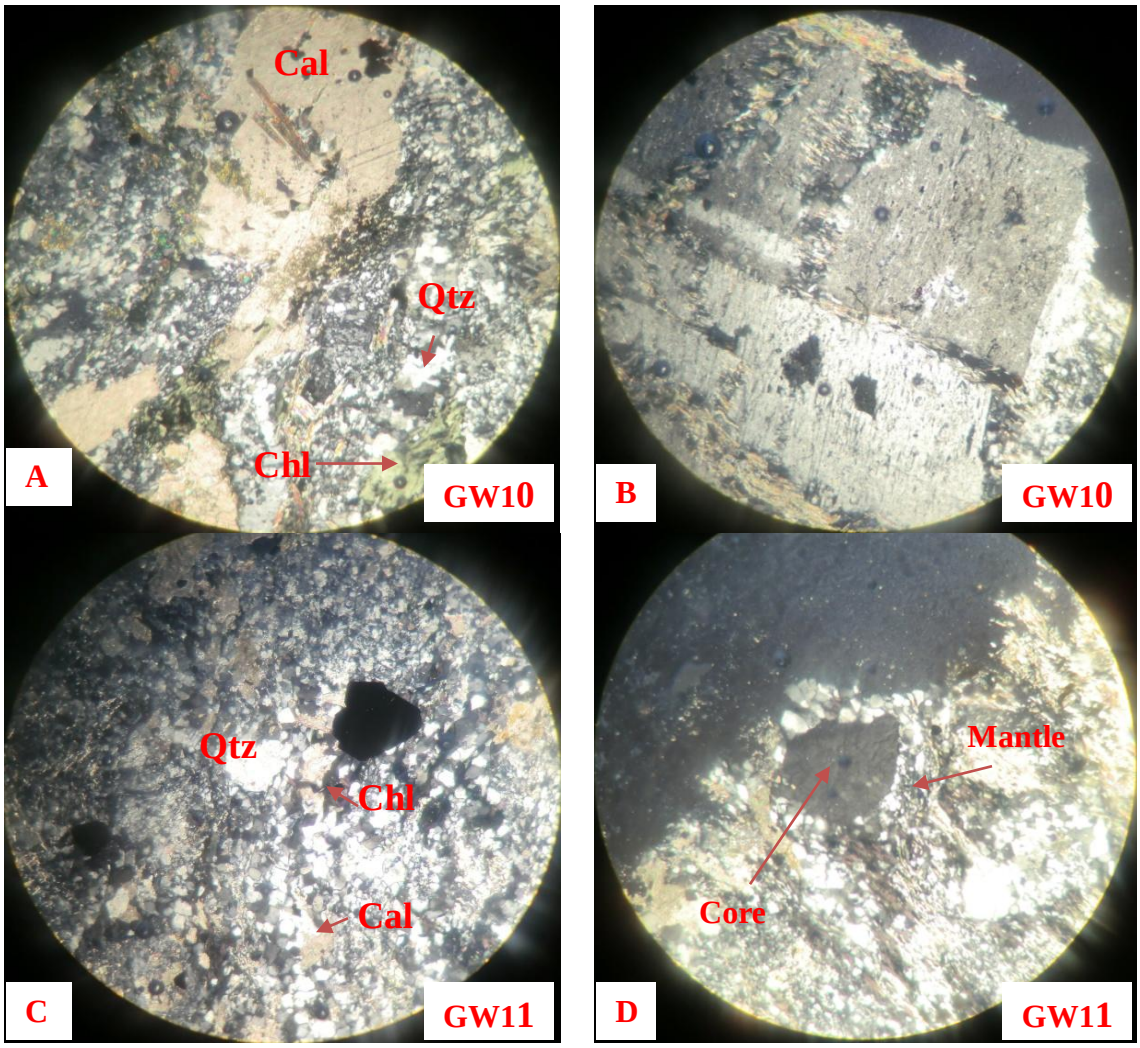


Figure 3.7 Photomicrograph showing different characteristics of minerals in metavolcanic breccias (observed under XPL). A) Larger calcite grains with inclusions of quartz B) The

same sample illustrating brittle fracture on quartz C) Quartz crystals of varying size and crystal moldic open space indicated by dark color. D) Core and mantle texture. Sample location; 0567134E, 1551897N (A and B), 0566708E, 1552215N (C and D). *Total magnification, 10x10=100x.*

The mineralogical composition of the rock is: 30% quartz, 25% calcite, 22% chlorite, 12% albitic plagioclase, and 9% opaques. Thus the name of the rock is: plagioclase-clorite-calcite-quartz metavolcanic breccia. Core and mantle structures in which the coarser quartz crystals are rimmed by the finer quartz grains /GW11/ (Fig. 3.7D). It is an indication of low grade metamorphism. It has a mineral assemblages of 35% quartz, 25% calcite, 17% chlorite, 15% muscovite, 8% opaque (pyrite?). Its name based on the abundance mineralogy is given as muscovite-clorite-calcite-quartz metavolcanic breccia.

### 3.5 PHYLITE

This rock found in the study area is characterized by fine grained low grade metamorphic rock with a phyllitic cleavage and it is found at the transition between the slate and the dolomite-slate intercalation. It shows strong S1 foliation having a shinny appearance because of the fine grained mica flakes and has peculiar undulating surficial features grayish in color. It is more crenulated than slates of the area at micro- and mesoscopic level creating crenulation lineation along its hinges. The unit has a thickness of about 38m which makes it the thinnest unit of the study area and it pinches out to the southern part of the area.

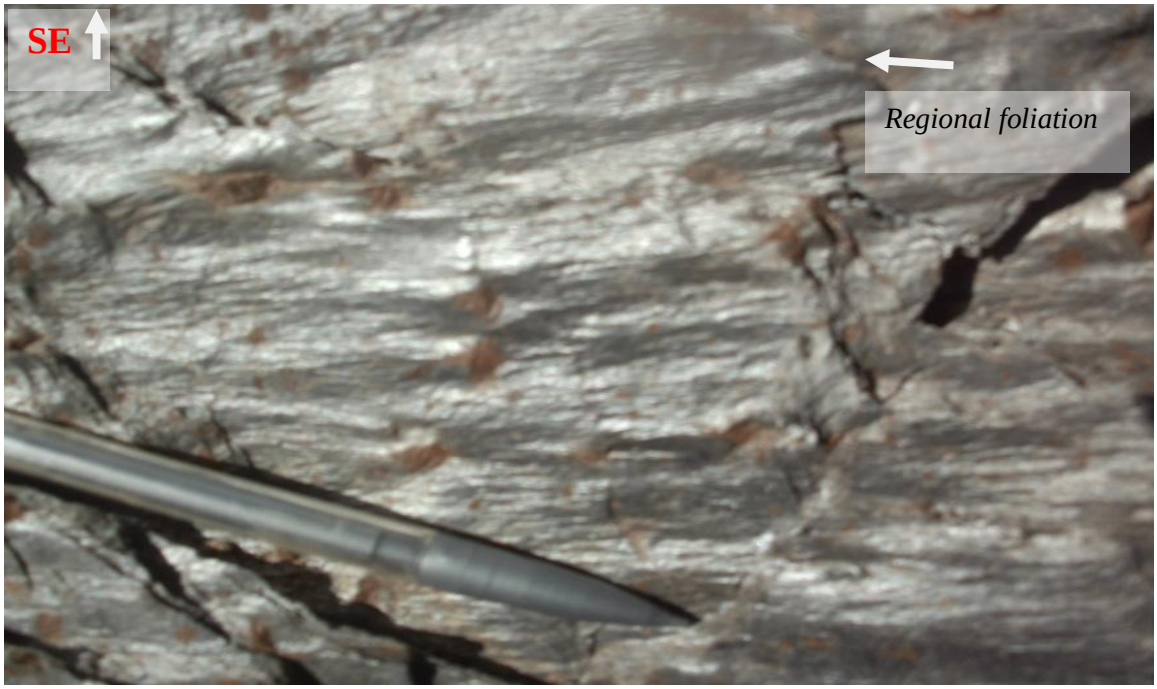


Figure 3.8 Field photograph of phyllite showing a shallowly plunging crenulation lineation. Orientation of foliation: $N14^0E/75^0NW$. Location; 0567923E, 1554242N. Direction of view is to the south east.

### 3.5.1 PETROGRAPHY

Sigmoidal shear sense indicators with a dextral sense of movements are observed on the porphyroblast (Fig. 3.9B) and porphyroclasts of the constituent minerals indicating that the rock is sheared to some extent. The shearing effect is observed displacing the fold hinges. Minerals mainly Muscovite, sericite, and deformed quartz are aligned parallel to $S_1$ foliation which is in turn crenulated perpendicular to the prominent regional foliation and formed $S_2$ foliation. Sericites in this rock are being altered into muscovites when it grades in to a higher temperature. Muscovite micas are the dominant phase in this rock. The protolith is rocks of a sedimentary origin where S1 foliation exist mimicking the primary $S_0$ foliation. Porphyroclasts of quartz minerals are dissolved on some parts of the rock with external fabric wrapped around the removed crystal moldic void spaces and the remaining quartz grains are fractured while some of them are recovering observed by their irregular boundaries with the adjacent minerals. Hence this pophyroblasts and

porphyroclasts of quartz crystals are pre-tectonic. The rock is composed of 35% muscovite, 30% quartz, 28% sericite, and about 7% of opaque grains and based on the constituent mineral aboundace, it is known as sericite-quartz-muscovite phyllite.

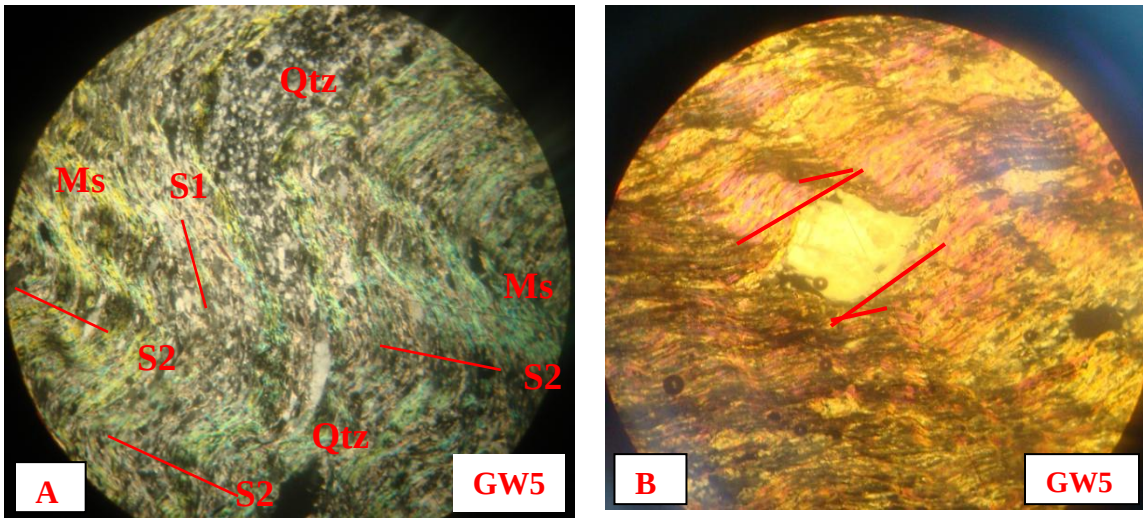


Figure 3.9 Photomicrograph of phyllite A) S1, Asymmetric crenulation cleavage S2, and compositional layering defined by alternating quartz rich and muscovite layers (observed under XPL). Total magnification 100x. Sample location; 0567923E, 1554242N. B) δ-Type Porphyroblast showing dextral sense of movement. *Total magnification; 10x10=100x*. Sample location; 0567923E, 1554242N.

### 3.6 META-DOLOMITE

The meta-dolomite units in the study area are commonly white and pinkish. Meta-dolomites with a pink color are found near the black meta-limestone and meta-dolomites farther to the western part of this limestone tends to be whiter in color. It is found intercalated with the slates in the meta-dolomite slate mixture zones of the mapped unit. This unit strongly preserved the evidences of tectonic activity in the area relative to the other units of the study area. Folds of various types open to isoclinals whose axis trends in different directions dominantly in the SW direction plunging at shallow to steep angle.

### 3.6.1 PETROGRAPHY

Very fine grained crystalline dolomites are the dominant phases in GW8/Fig 3.10B/ showing primary bedding. It indicates deep burial diagenesis formed replacing finer calcitic sediments and metamorphosed later. They are formed at the mixing zone between the continents and sea water where water from the continental areas containing $Mg^{2+}$ mixed with calcites from sea water replacing $Ca^{2+}$ and latter buried to high depth indicated by laminar cleavages of calcite crystals. Planar and mostly subhedral dolomites are abundant in GW4/ Fig 3.10A/. Open spaces are found formed when calcites are replaced by dolomites because the dolomite minerals are compacted and occupy less space compared to the calcites and they shrink into dolomites leaving voids between the grains.

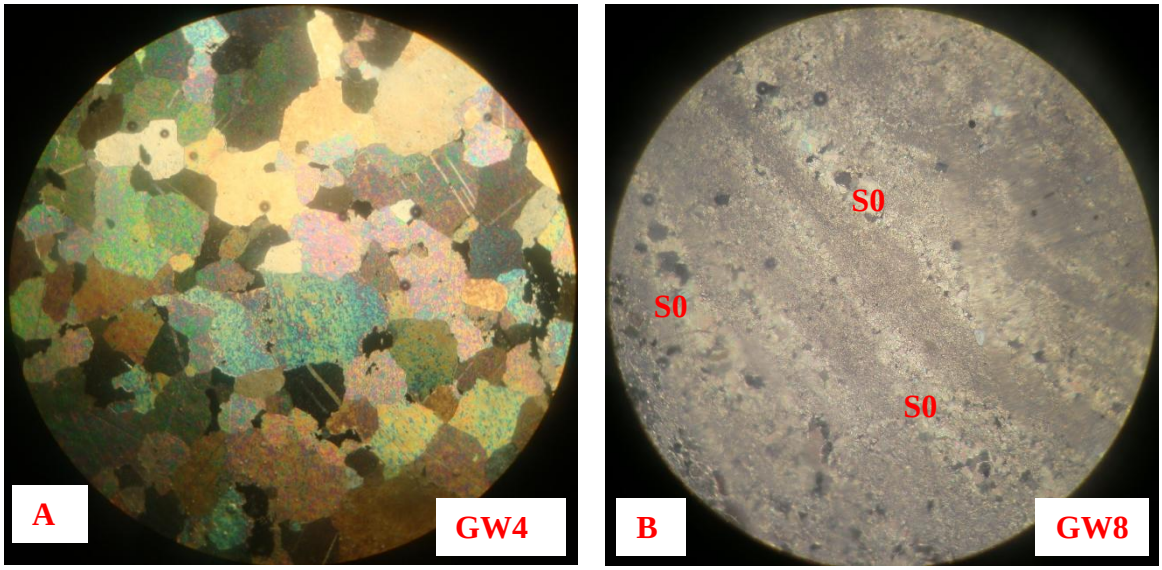


Figure 3.10 Photomicrographs of dolomite. A) Planar and subhedral dolomite crystals (observed under XPL). B) Primary bedding S0 on crystalline dolomite (observed on XPL). *Total magnification; 10x10=100x*

## 3.7 META-DOLOMITE AND SLATE INTERCALATION

The Meta-Dolomites and slates are intercalated to form one major lithological unit of the study area. The unit is found right after the phyllite when going to the east towards the

basin. The unit is either dominantly meta-dolomite or dominantly slate forming the intercalation. Looking from far the cliff of this unit, the meta-dolomite stands stiff from its surrounding weathered slate because of its competence to weathering relative to the slate. Later formed quartz, tourmaline, and aplite dikes running in different direction with some of the major thicker E-W aligned veins of quartz crosscutting the unit specially the dolomite rocks. The unit dominates the study area covering much of the area and it is thicker than other units of the study area.

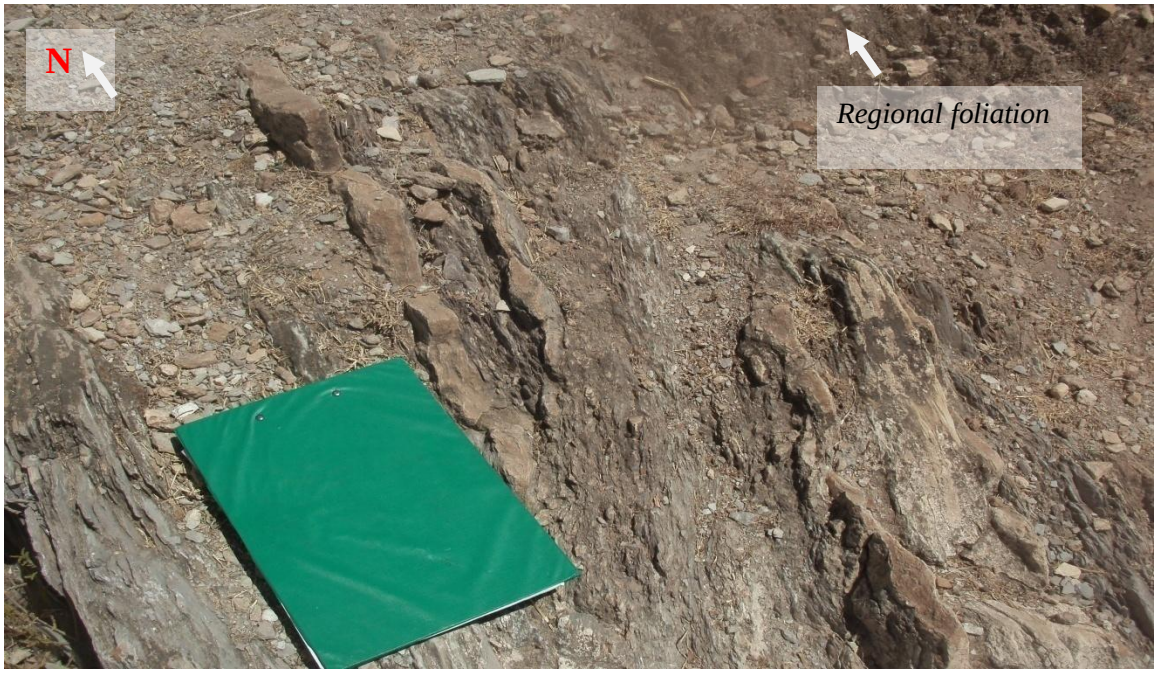


Figure 3.11 Field photograph of meta-dolomites intercalated with slate and it has orientation of N30E/40NW. Location: 0570478E, 1550981N. Direction of view is to the North.

### 3.8 META-LIMESTONE

The Meta-limestone is found at the eastern boundary of the study area. It is fine grained, hard, highly compacted and black in color. The average orientation of this unit is NE-SW. The unit is highly crosscut by quartz veining with no systematic pattern. It less weathered compared to the adjacent units. The unit shows primary bedding and forms high altitude ridge with a very steep topography at the bottom of basin.


Figure 3.12 Primary bedding $S_0$ on Black meta-limestone found at the eastern part of the study area. Attitude of $S_0$: N30E/55SE. Location: 0570347E, 1548736N. Direction of view is to the SE

### 3.8.1 PETROGRAPHY

Fine grained micritic calcites (see Fig 3.13) characterizes this rock and they are the dominant phase containing two generation of calcite veins with two parallel sets of calcite veins cross cut by younger and thicker vein (Fig 3.14F). The rock is neomorphosed to form sparry calcites. Evidences of latter deformation is seen by laminar cleavages of calcite in which one sets cleavage making the calcite crystal orthorhombic is usually absent or very faint because of deformation. Micritic calcites are slightly aligned due to the earlier deformation and the larger calcites in the vein formed later and grow larger because of enough spaces in the vein. Then later came another phase of deformation after the crystallization of calcites in the vein. Its mineralogical composition is: 92% calcite, 5% quartz, 3% insoluble material.

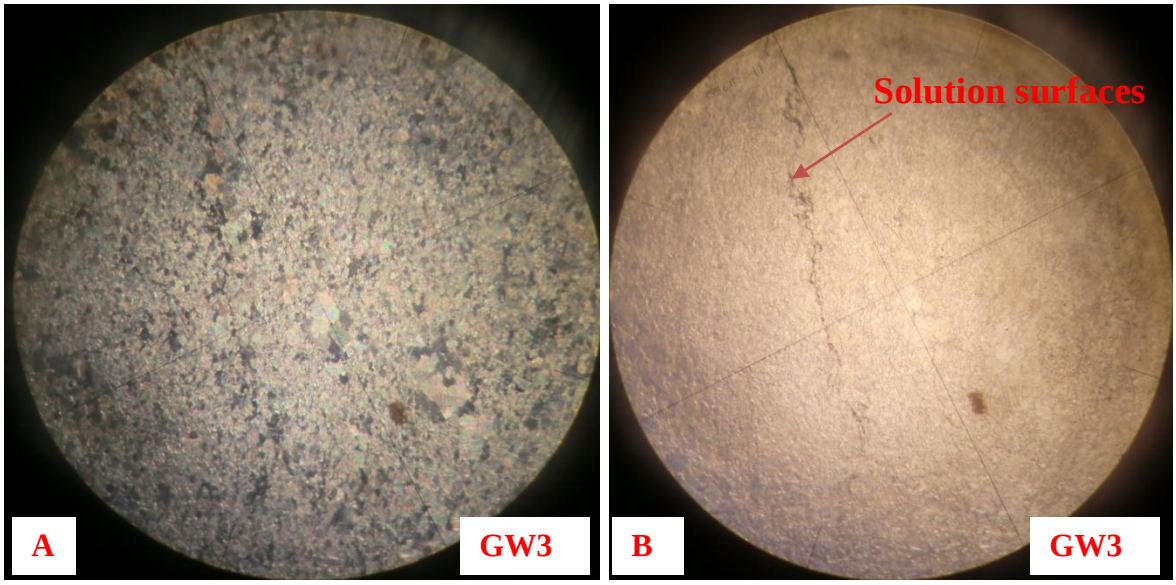


Figure 3.13 Photomicrographs of limestone from the same sample. A) Micritic calcite observed under XPL. (B) Solution surface along the boundaries of calcite crystals. *Total magnification; 10x10=100x.* Sample location; 0571115E, 1551809N.

### 3.9 PHANEROZOIC SANDSTONE

This is the younger formation of the Phanerozoic age usually found overlying the oldest Neoproterozoic rocks of the study area showing angular unconformity with them. The western boundary of the study area is bounded by this units and it is also found at the southern part of the area overlying the slate and dolomite-slate intercalation. It is characterized by visible medium grain texture and white color. Red sandstone is also encountered on some of the area with a high iron content which gave them a red color. Encrustation is a common feature observed on this sandstone. The unit generally trends in the N-S direction having almost horizontal bedding unlike the Precambrian age units of the study area.

### 4.10 VEINS

Veins are found both at microscopic and mesoscopic scale. Quartz veining dominates the veins although there are fewer and thinner tourmaline veins are observed which are usually found on the slates parallel with its foliation along the strike. Intense quartz and

associated pyrite (?) mineralization is observed on the veins specially around Guims Kebele of the Guwila area at the south western part of the study area and the thickest quartz vein is also measured on this area. It is found on the meta-volcanic breccia and is about 70cm wide trending 085/80SE with a nearly vertical dip angle and is discordant to regional foliation cutting the unit across the strike (Fig. 3.14A).

N-S trending quartz veins are found on some of the places which are concordant with the main foliation (Fig. 3.14B).

Microscopic examinations of rocks indicate that there are veins of different character. Thin section GW3 has calcite veins with two different generations one crosscut by the other (Fig. 3.14F). The calcite veins which are parallel with each other and run parallel with the outer fabric cut by the other thicker vein. The calcites in the vein, however, is discordant with the outer fabric. The growth of calcites in those veins can be described as syntaxial in which the growth starts from the wall of the vein to the center of the vein.

Some of the quartz veins are folded by the later shearing forces applied oblique to the foliation plane. Finer inclusions are observed in calcites which are probably fragments from the wall rock.

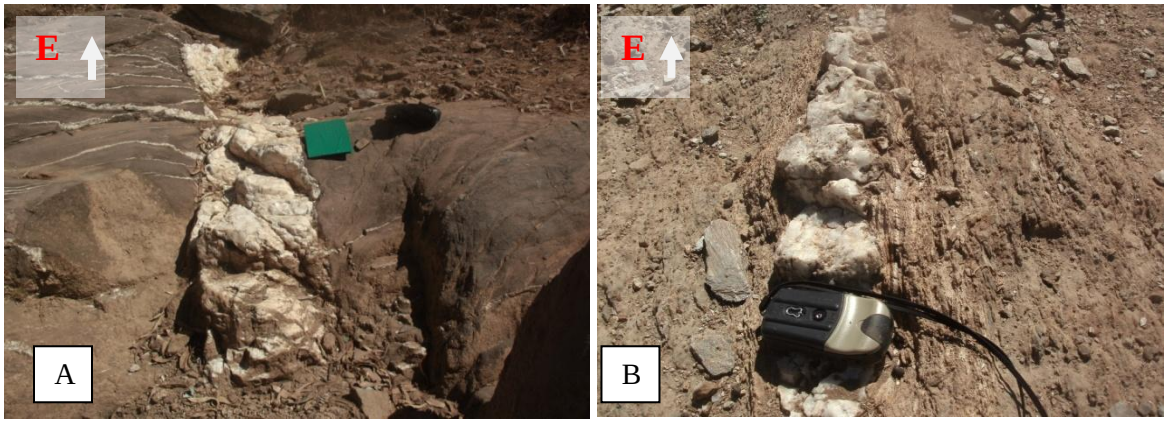

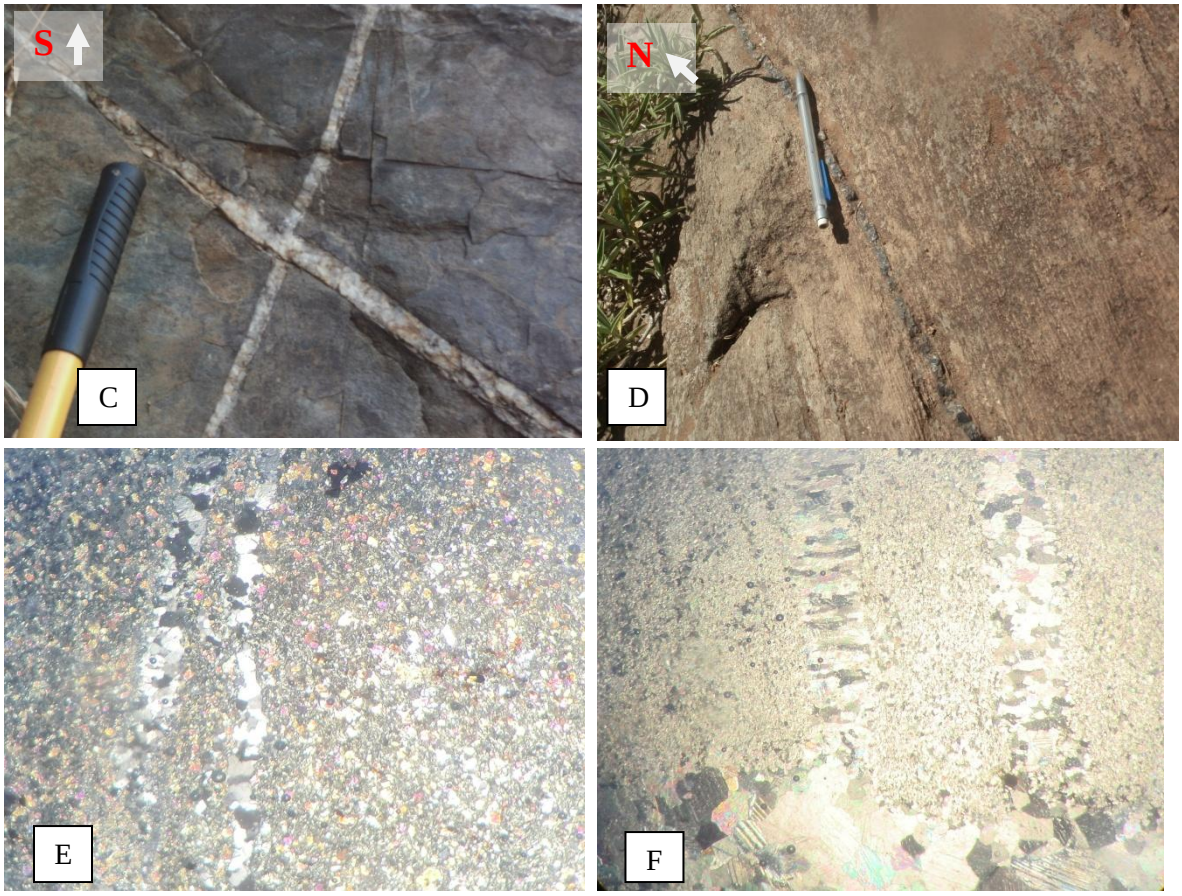


Figure 3.14 Quartz and tourmaline veins A) Discordant quartz vein on the meta-volcanic breccia. Direction of view; East B) Concordant quartz veins on the slate C) Two generations of quartz veining, N30W/45SW relatively thicker and the other trending N20E/60SE. From the crosscutting relationship on the field, quartz vein trending NE/SE is cross-cut by the NW/SW, hence it is probably older. Picture taken facing to the south. D) Tourmaline vein trending N5E/70SE parallel with the regional foliation. E) Photomicrograph showing quartz veining (GW9) Total magnification; 10x10=100x F) Photomicrograph of two sets of calcite veins (GW3). Total magnification; 4x10=40x.

# CHAPTER – IV GEOLOGICAL STRUCTURE AND DEFORMATION

## 4.1 INTRODUCTION

The metamorphic rocks of the study area have been subjected to ductile and brittle deformations. Although the regional structural frameworks are used to interpret the main deformation fabric elements, close examination of the characteristics in the field and microscope were carried out to identify the general deformational history of the study area. Field measurements of foliation, lineation, fold axes, interlimb angles of folds, etc are used to group geological structures of the study area in to different generations. At least two phases of deformations are found in the area.

## 4.2 HISTORY OF DEFORMATION

### 4.2.1 D1 DEFORMATION

#### *4.2.1.1 F1 FOLDS*

D1 is responsible for the formation of F1 folds which are commonly preserved on the metadolomites of the study area. They are usually encountered on the meta-dolomites and are one of the common diagnostic structural elements associated with D1. These kinds of folds are easily identified on the field by their steeply plunging axis and low interlimb angle. F1 folds are irregularly distributed on the study area. They are tight to isoclinal with a measured interlimb angle of less than $20^0$ plunging $50^0$ to $80^0$ in various directions (Fig 4.2A-C).

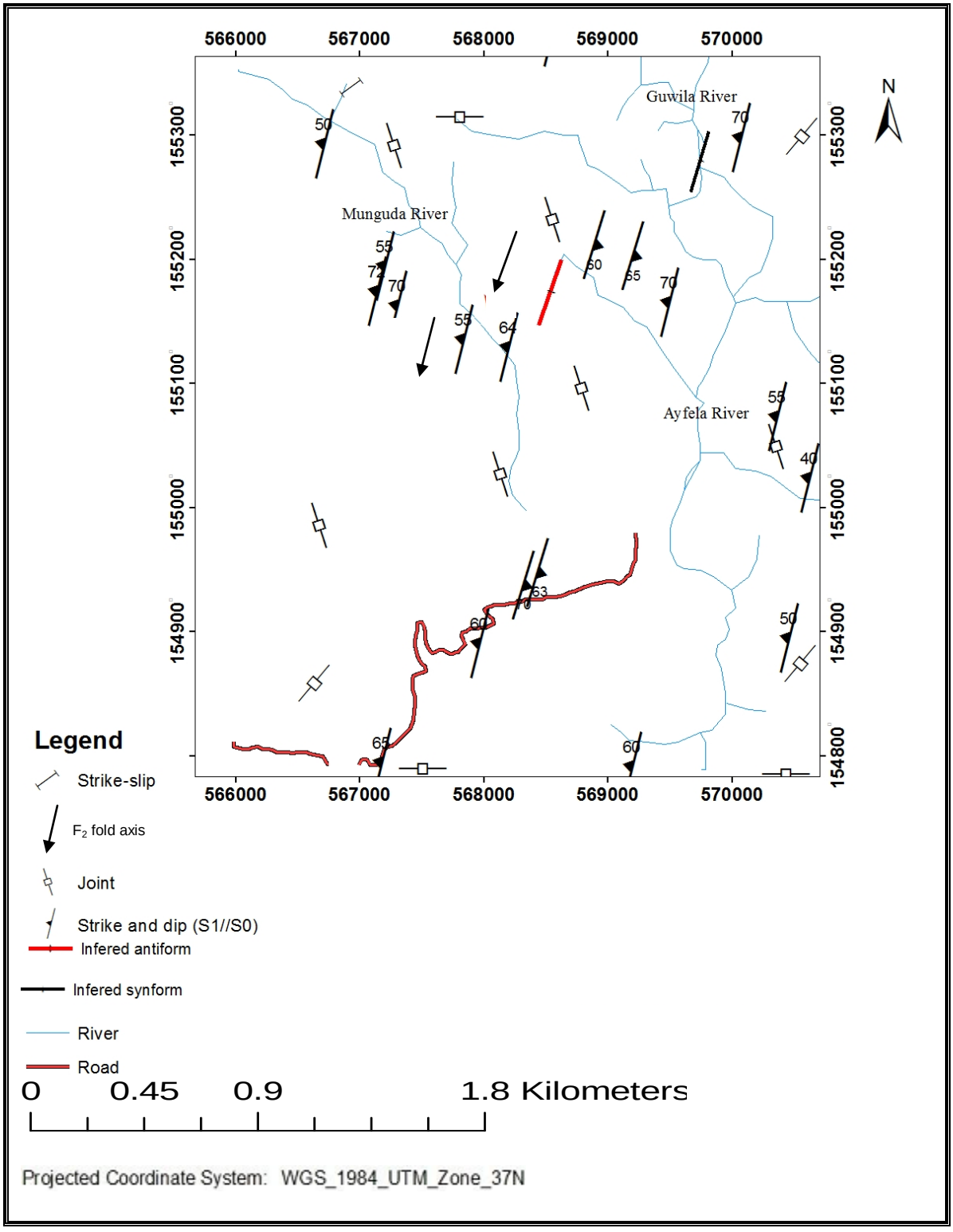


Figure 4.1 Structural map of the study area

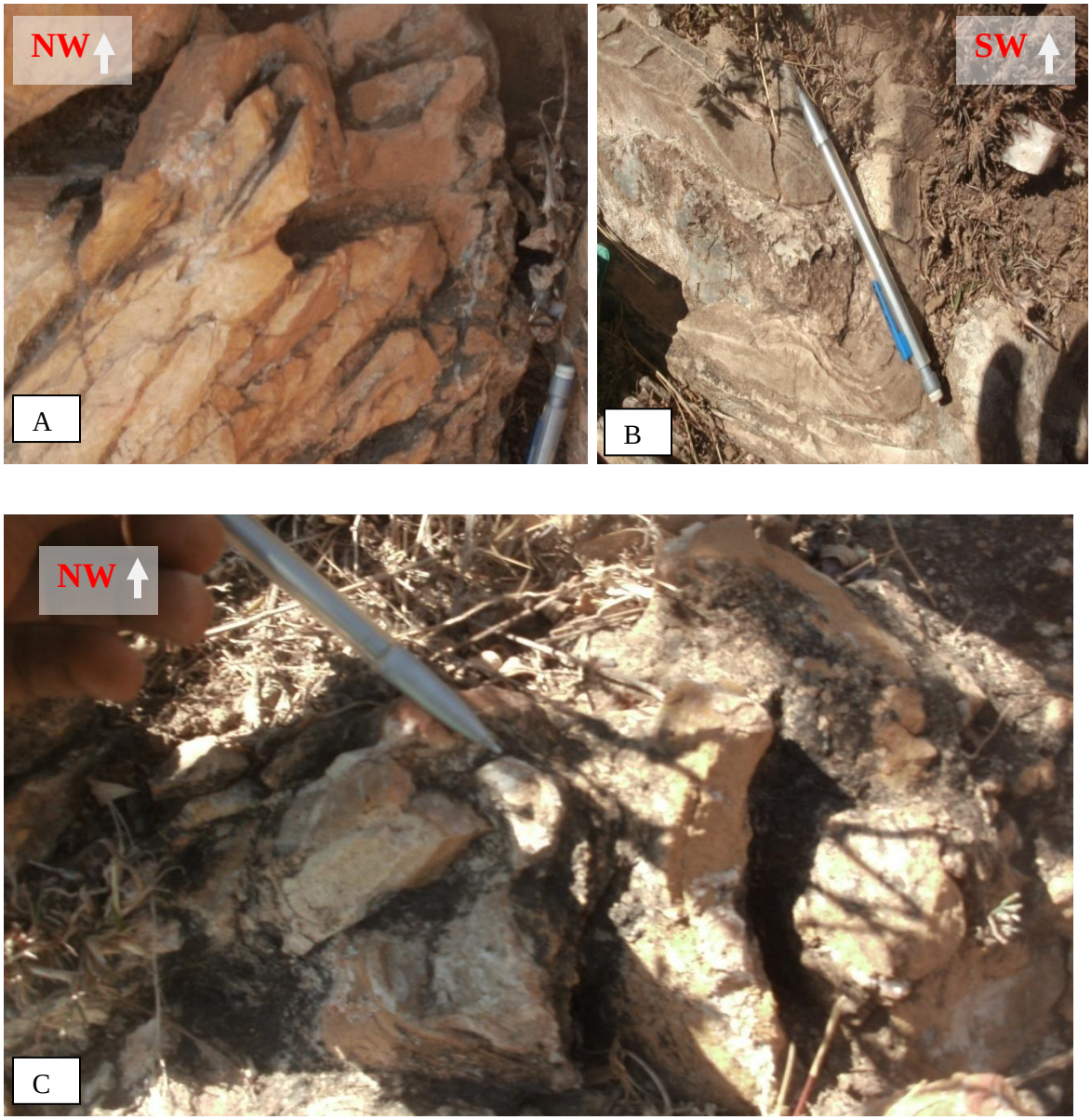


Figure 4.2 Field photos of first generation F1 folds. A) Isoclinal fold with fold axis plunging $78^0$ SE. Direction of view is to the NW. Location; 0570478E, 1550981N. B) Tight folds with fold axis plunging $50^0$ SW. Direction of view is to the SW. Location; 0567301E, 1551780N C) Fold with a characteristic feature of reclinal, and angular hinge and plunging $80^0$SE. Direction of view is to the NW. Location; 0570478E, 1550981N.

*4.2.1.2 S1 FOLIATION*

The first phase of deformation is characterized by the formation of pronounced regional $S_1$ foliation (Fig. 3.2, 3.8, & 4.3). Penetrative S1 foliation is well developed on metasediments and under petrographic examination, it is represented by parallel alignment of their constituting minerals commonly, sericite, muscovite and quartz. And it is also developed parallel or sub-parallel to the original layering/bedding S0.

$S_1$ is a major foliation with a dominant strike direction of NNW/SSE to NNE/SSW and dipping 60 W and E. The variations may be attributed to the later phase of deformation. -


Figure 4.3 Field views of the main regional foliation (S1) developed on the slate whose attitude is N20E/60SW. Location; 0568194E, 1552065N. Direction of view is to the North.

The variation of dip direction is an indication of the presence of alternating synforms and antiforms as a result of later deformation (D2).

The plotted foliation measurements are concentrated on nearly two regions of the Lambert projection, in the second and fourth quadrants (Fig. 4.9).

*4.2.1.3 L1 STRETCHING LINEATION*

This kind of lineation is characteristically found on the volcanic-breccias defined by closely packed elongate clasts forming linear patterns. They usually plunge at a shallow angle due to the D2 deformational event. The average trending direction of this lineation is ENE-WSW (Fig. 4.4A & B).

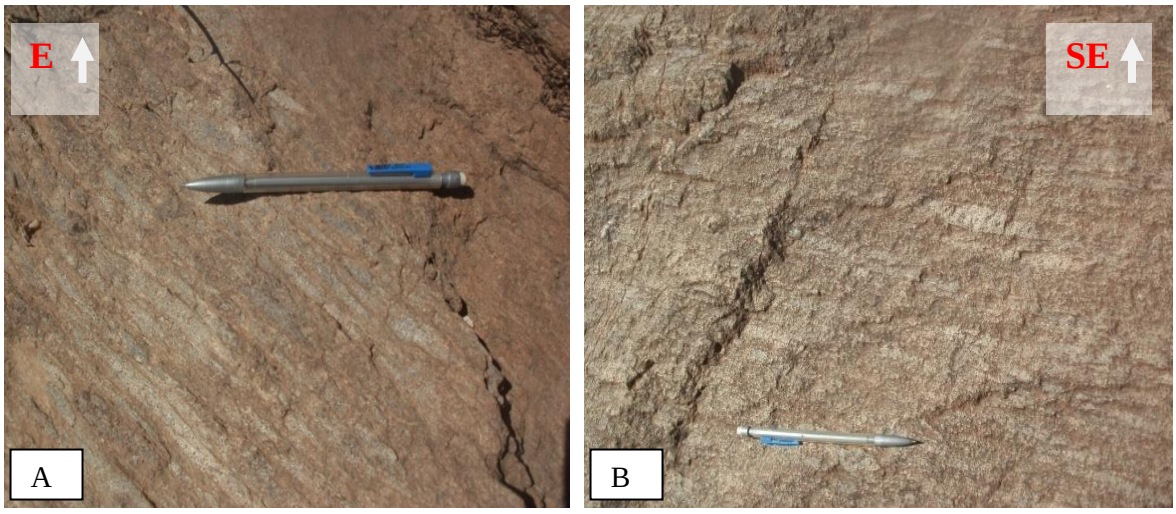


Figure 4.4 Field photos showing L1 lineations from metavolcanic breccia. A) L1 defined by stretching pebbles ($40^0 \rightarrow 095^0$). Picture taken facing to the east. Location; 0567114E, 1551843N. B) Stretching lineation L1 ($23^0 \rightarrow 086^0$). Picture taken facing to the south east. Location; 0567114E, 1551843N E).

4.2.2 D2 DEFORMATION

*4.2.2.1 F2 FOLDS*

These folds have a much larger wavelength and interlimb angle compared to folds formed by D1 deformation (Fig. 4.5A-F). Larger Interlimb angle opening up to approximately $170^0$ measured near Agamat Maryam church on the slate (Fig. 4.5D). All

kinds of D2 folds in the area have nearly horizontal shallow plunging fold axis with their fold axial plane either sub horizontal (those which are overturned) or sub-vertical (antiformal and synformal).

Axial plane of the F2 folds are generally parallel with the pervasive regional foliation S1 of the area. The crenulation lineation and the mineral lineation measured from the field are also found to be parallel with the fold axis of F2 folds. Meta-dolomites of the study area preserved both phases of deformation (Fig 4.6A-K).

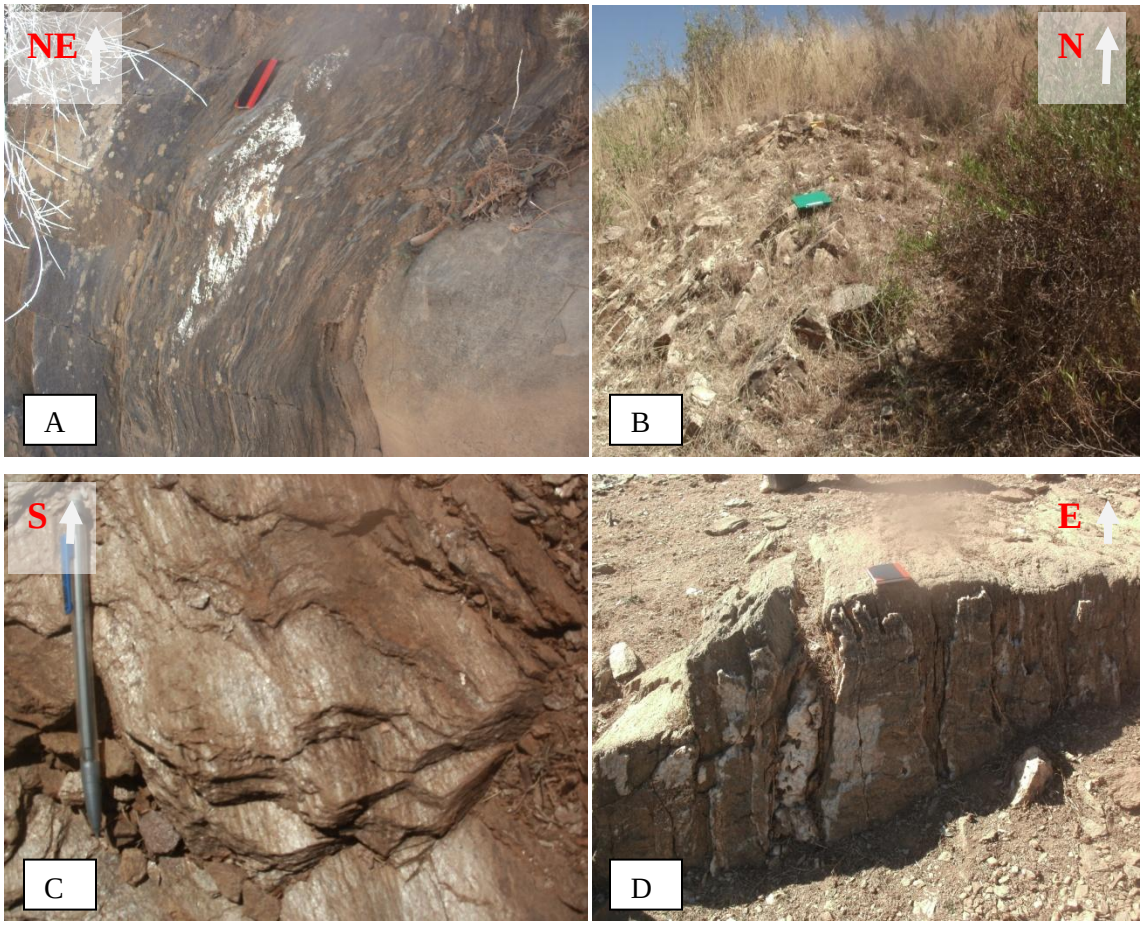


Figure 4.5 F2 Folds measured from different localities of the study area. A) Recumbent folding on slate. Axial plane N-S/10$^{O}$E. Direction of view- NE. Location; 0566948E, 1552503N. B) Upright fold with wider interlimb angle having a gently SSW plunging fold hinge. Picture taken facing north. Location; 0567421E, 1550904N. C) Crenulated foliation forming upright fold with a relatively shorter wavelength of about 10cm and amplitude of about 2.5cm. Axial plane; N12$^{O}$E/71SE. Fold axis; 7$^{o}$→012$^{o}$. Direction of view is to the south. D) Open fold on slate with horizontal axial plane whose interlimb angle is 170$^{0}$. Direction of view is to the east. Location; 0566765E, 1552623N E) Open fold whose axial plane is N8$^{O}$W/5$^{O}$NE. It is kinked and has an interlimb angle of approximately 120. Direction of view is to the south. F) Upward facing fold on black limestone whose axis dips at shallow angle. Direction of view is to the south. Location; 0571086E, 1553840N.

*4.2.2.2 SUPERIMPOSED FOLDS*

Superimposed ductile deformations are often observed on the meta-dolomites of the area (Fig. 4.6A-K). Early formed tight to isoclinal folds are refolded about the same axis and produced type 3 interference pattern which looks like a 'hook'. Meta-dolomites preserved both phases of folds at an outcrop scale unlike other units in the study area. It is possible to trace the axial plane F1 and F2 from those folds and individual phases are identified on the field. Axial plane of F1 folds are folded by F2 folds whose axial plane trending in various directions. F2 folds are superimposed on folds of earlier generation F1.

A

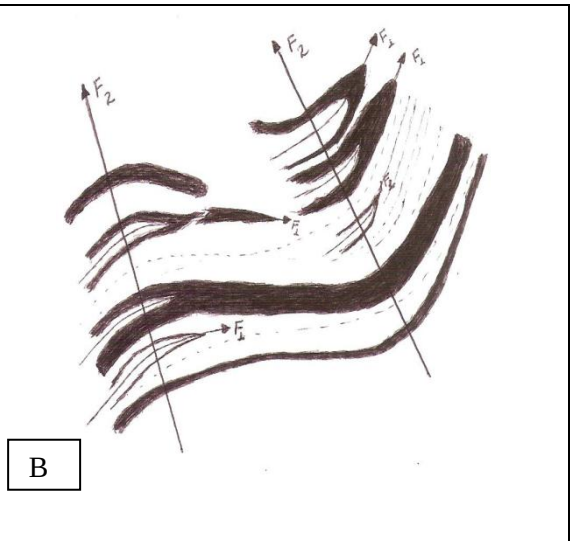


B

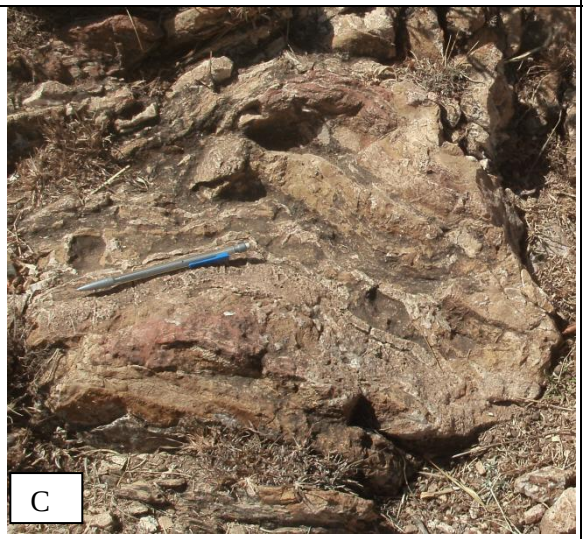

C

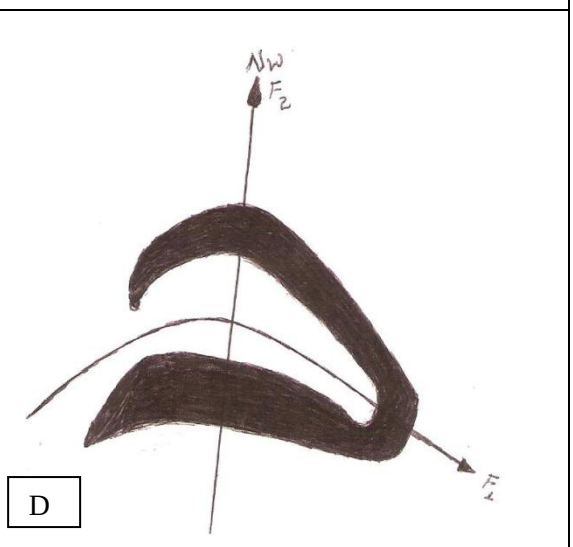


D

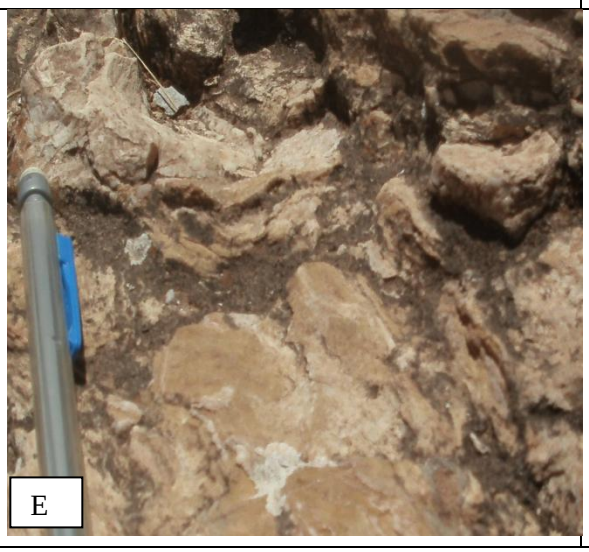

E

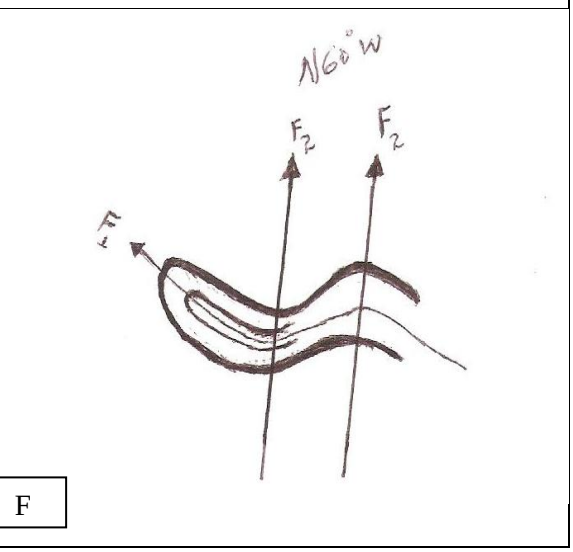


F

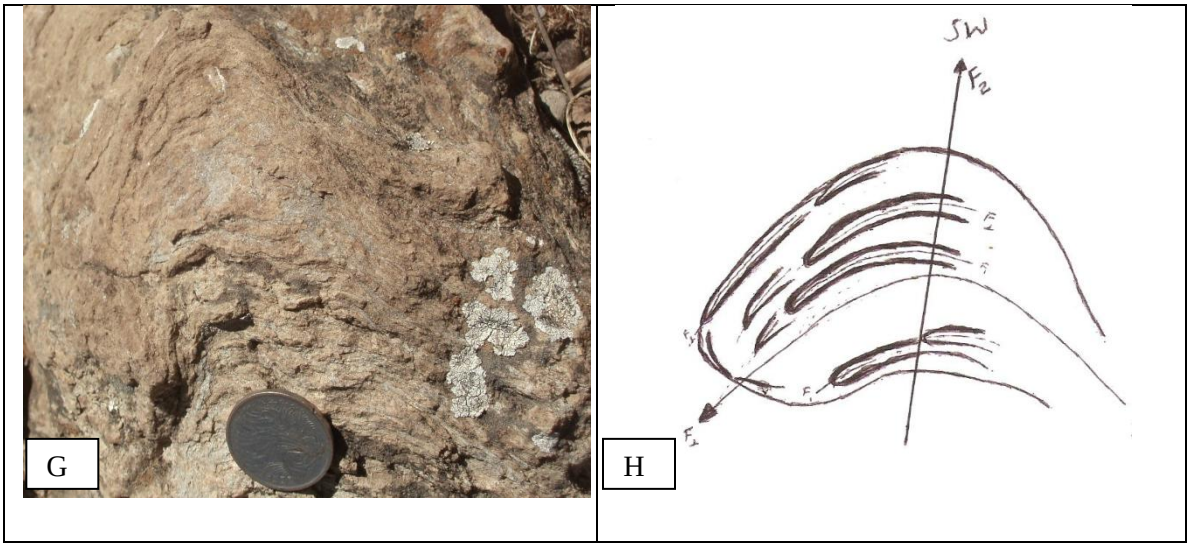
G
SW
F2
H

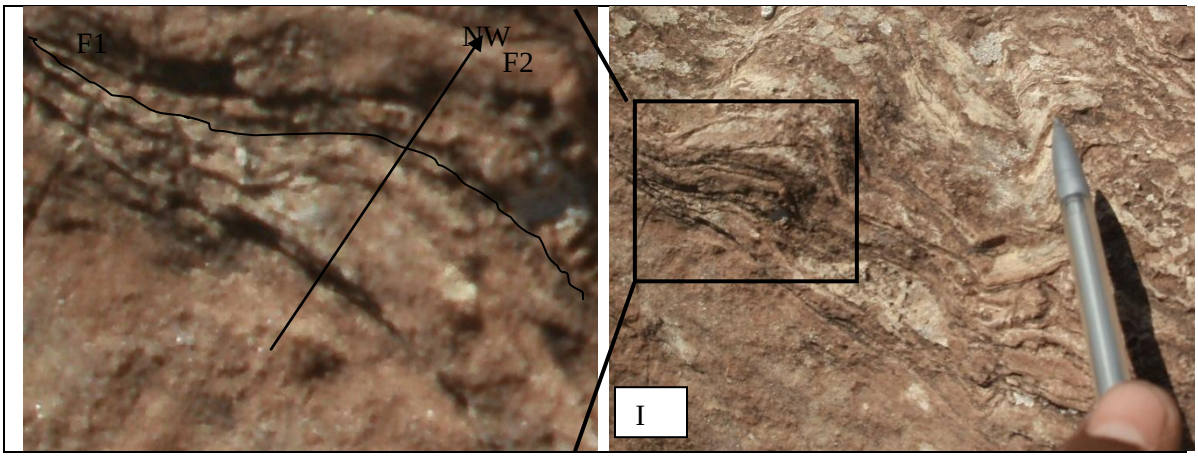
F1
NW
F2
I

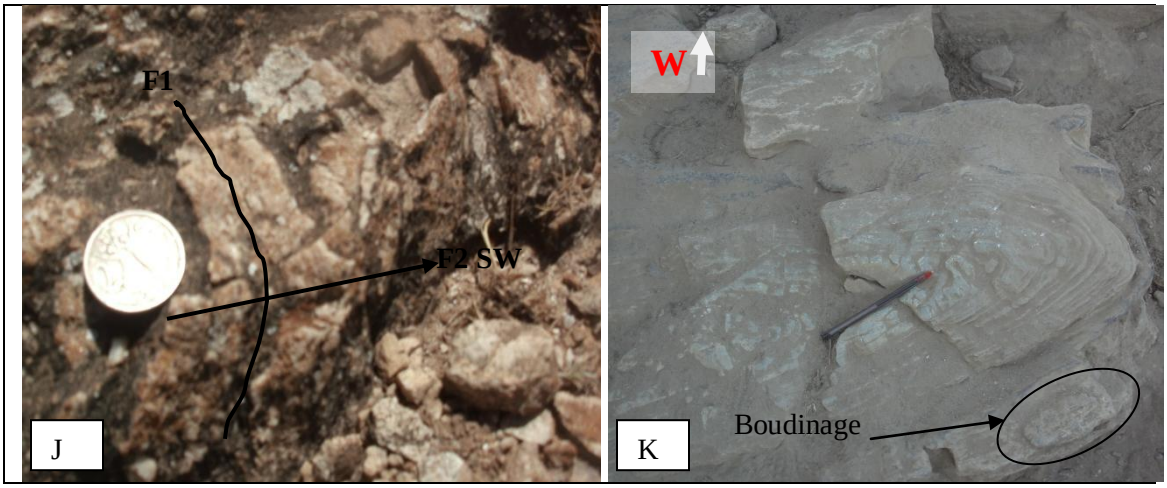
F1
F2 SW
J
W
Boudinage
K

Figure 4.6 Super imposed folds. B, D, F, and H are hand sketches representing A, C, E and G respectively. (A and B) Fold showing two phases folds F1 and F2. It could be described as Type 3 interference pattern. (C and D) F2/trending NW folds is poorly developed because the thicker competent dolomite layer. Fold axis of F1 is folded. The fold resembles type 3. D/n of view is to the west. (E and F) Orientation of axial plane of F2 fold can be measured: N60$^{O}$W70NE. Direction of view is to the North. (G and H) The morphology of this fold is relatively closer to Type 3 fold than the others. The average axial plane of the F1 fold is indicated on the figure H is folded D2 responsible the formation of F2. Direction of view- South I) Refolding on harmonic fold with common axial plane of second phase F2 generally trending NW. Picture taken facing west. J) F2 of this fold trends in the SW. Picture taken facing east. K) Refolding of vertically plunging fold showing boudinage as indicated on the figure. Location; 0570478E, 1550981 (C, E, G, I, J), 0567413E, 1551863N (A and K).

#### *4.2.2.3 S2 FOLIATIONS*

S2 foliation is traced along the crenulation surfaces of phyllites (see Fig. 3.9 & 5.1B) and slates (faintly developed at microscopic scale) and is nearly perpendicular to S1 foliations when its surface is crenulated.

Plots of foliation data collected from the area on the stereogram indicate that there is a well developed fold whose fold axis generally trends in SW direction and there is approximately WNW-ENE directed stress which folded the S1 foliation (Fig. 4.9).

#### *4.2.2.4 L2 CRENULATION LINEATIONS*

They are found at the fold hinges of rocks crenulated during an approximately layer parallel stresses during D2 deformation. They are well developed on phyllites and volcanic breccias and they dominantly plunge $8^{0}$ in the SW direction (Fig. 3.8, 4.7A & B). It is usually seen forming an array of straight, discontinuous crests and troughs of minor crenulated folds.

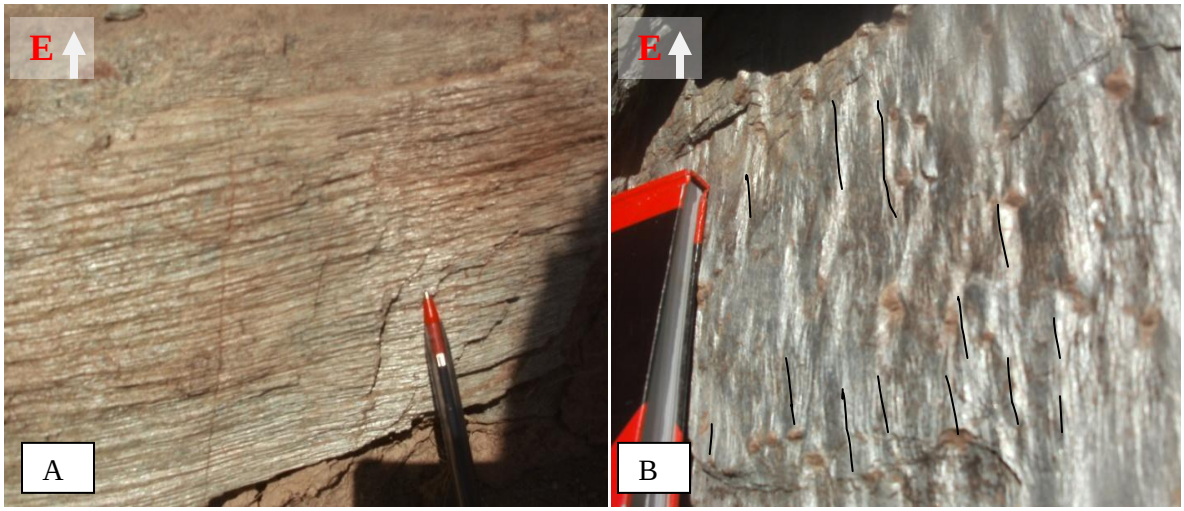


Figure 4.7 Field photos showing L2 lineations. A) Crenulation lineation L2 ($5^0 \rightarrow 195^0$) on metavolcanic breccias. Picture taken facing to the east. Location; 0566708E, 1552215N B) Crenulation lineation on phyllite. Picture taken facing to the east. Location; 0567923E, 1554242N.

### 4.3 JOINTS

There are generally three sets of joints trending in the NW-SE, NE-SW, and EW directions having a shallow to steeply dipping inclination angle.

Closed, open and crosscutting joints are observed on the field. Some of the open joints have infillings of secondary materials such as silica precipitates. All of the units of the area have joints emphasizing that the latter brittle deformation is wide spread covering the entire portion of the area and they are considered as D3 deformation phases.

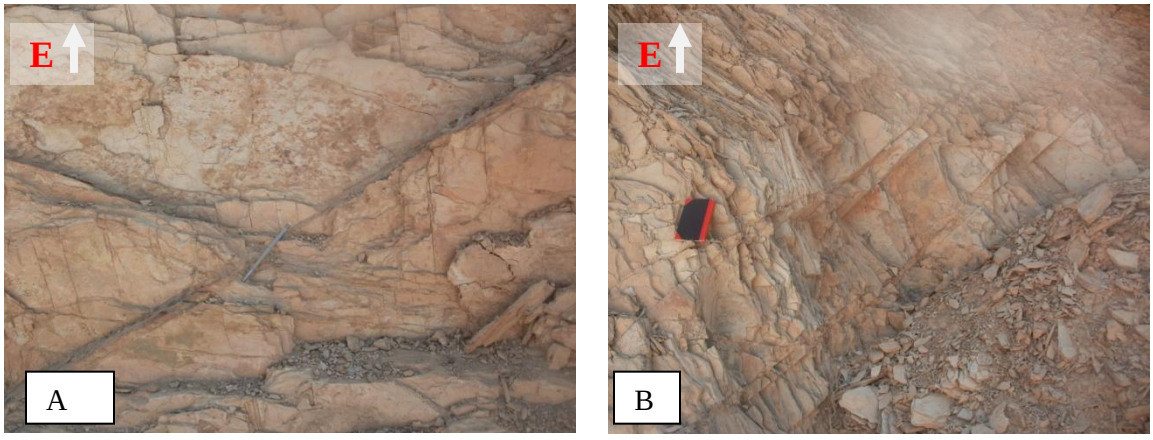

Figure 4.8 A) Joints on the slate with E-W/25N orientation B) joint system on slate. Picture taken facing to the east.

## 4.4 PRESENTATION OF STRUCTURAL DATA ON EQUAL AREA NET AND ITS ANALYSIS

Spatial data collected from the field are plotted on equal area net for structural analysis and interpretation. The software used is Stereonet8 developed by Rick Allmendinger (2013). Lower hemisphere spherical projection onto a horizontal plane is applied on the equal area Schmidt net to describe the final interpretation of geometrically oriented structural elements measured on the field along with the field analysis of its nature and its characteristics on the structural map.

Both planar and linear structural entities show some meaningful concentration along certain areas. Poles to foliations calculated from N=59 measurements show a cluster of mainly two regions (Fig 4.9), on the second and fourth quadrants of the stereonet. The planar data plot of these foliations indicates that it generally dips in two directions dominantly in the NW and SE. From this it is possible to interpret the presence of large scale folds in the study area. It will be biased, however, to designate the fold as either antiformal, synformal or alternating synformal and antiformal by using the equal area projected data because the plot generally gives us two dipping direction in all of the above cases. Field analyses of the foliations indicate change in the dipping direction of the foliation in a short distance along the E-W traverse line implying the change in the facing direction of the fold.

Kamb method is used for contouring the foliation data because it smoothes out the contour irregularities that are of no statistical significance (Fig 4.9B) and Figure 4.9C shows 1% area contouring for comparison. The general trend of this foliation indicates that it is folded by approximately WNW-ESE directed stress whose fold axis trends SSW. The fold can be generally classified as upright whose axial plane dips steeply and because the axial plane of the fold inclined steeply and its axis plunges shallowly, it is more appropriate to call the fold upright plunging.

There are a number of intersection points on the plots of planar foliation measurements in which two foliations intersect at a certain part of the region. About 1711 intersection points calculated from 59 foliation measurements leading us to maximum concentration of β intersection points (Fig 4.10D). The intersection points in general are concentrated in two different regions in the SW and NE specially of those dipping in two opposite directions NW and SE. Thus there are two β-axis, major and minor and because the majority of the intersection points are concentrated on the third quadrant, they define major β-axis that coincides with the π-axis which is the pole of foliation girdle. The mean of β-axis is statistically parallel to the fold axis (Ramsay, 1967), hence, they can be considered as the fold axis of the major fold.

The distribution of poles on the Schmidt net and the symmetry of the pattern of its contours can give us a clue on the form of the fold. The maxima on the π-girdle correspond to two limbs and are concentrated on two different regions. From this we can conclude that the fold has a narrow hinge.

Other planar structures such veinlets, and joints are plotted to characterize their general orientation in relation to foliations (Fig. 4.11). Plots of poles to joint surfaces are found scattered on the Schmidt net on all over the region but closely observing, they show some arrangements more concentrated in the second and fourth quadrant. Generally about two sets of joints can be identified, NW trending and NE trending.

Equal area nets are also useful in analyzing fabrics. They are used to calculate the true orientation of fabrics and to describe the variations in geometry of fabrics that occur between different domains of fabric. Measured data of linear fabric shows a systematic arrangement when plotted on the net in which most of them are clustered in the third quadrant i.e. trending in the SW direction (Fig. 4.10C &D). Fold axis and the majority of the lineations shows a parallel alignment with each other both of them plunging in the SW at a very low angle. The fold axis denoted by no.3 on the Schmidt net (Fig. 4.9) represents the hinge lines of the major D2 folds. Therefore the fold plunges in the south west direction at low inclination angle from horizontal. Unlike the crenulation lineation, flexural lineations formed by stretching pebbles show different pattern and are clustered on the eastern part of the region.

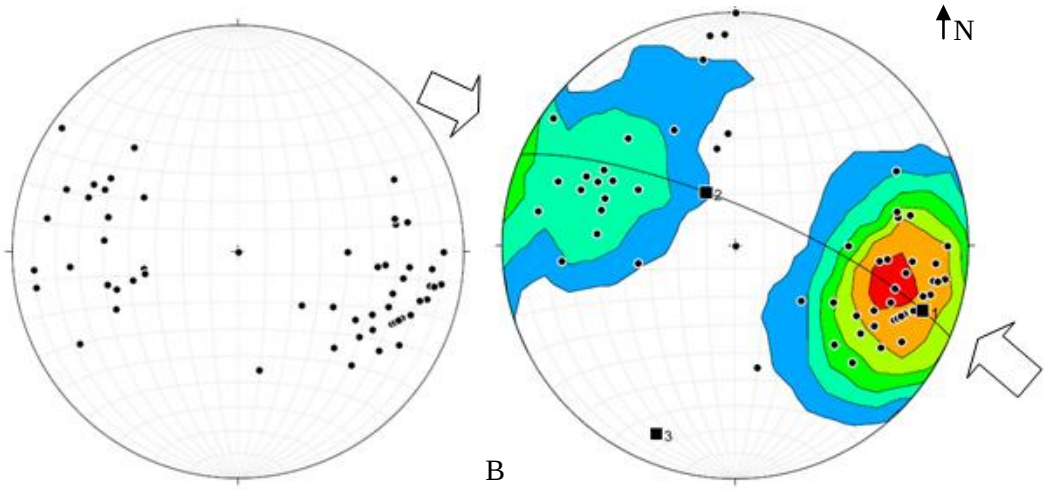


A B

Kamb Contouring-----
Data set name = poles to Foliation
Contour Interval. = 2 sigma; Counting Area = 0.% of net area
Expected Numuber. = 0 Signif. Level = 3 sigma

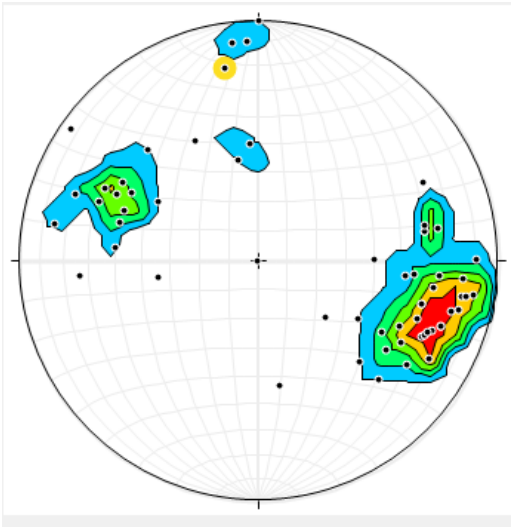


C

1% Area Contouring-----
Data set name = poles to Foliation
Contour Int. = 2%; Counting Area = 1% of net area

Figure 4.9 A) Plots of pole to foliation B) Kamba contouring with a cylindirical best fit or π girdle whose pole (***$14^0 \rightarrow 203^0$***) is denoted by number 3 at the third quadrant. C) 1% Area Contouring of the same data.

*No. Data: 59*

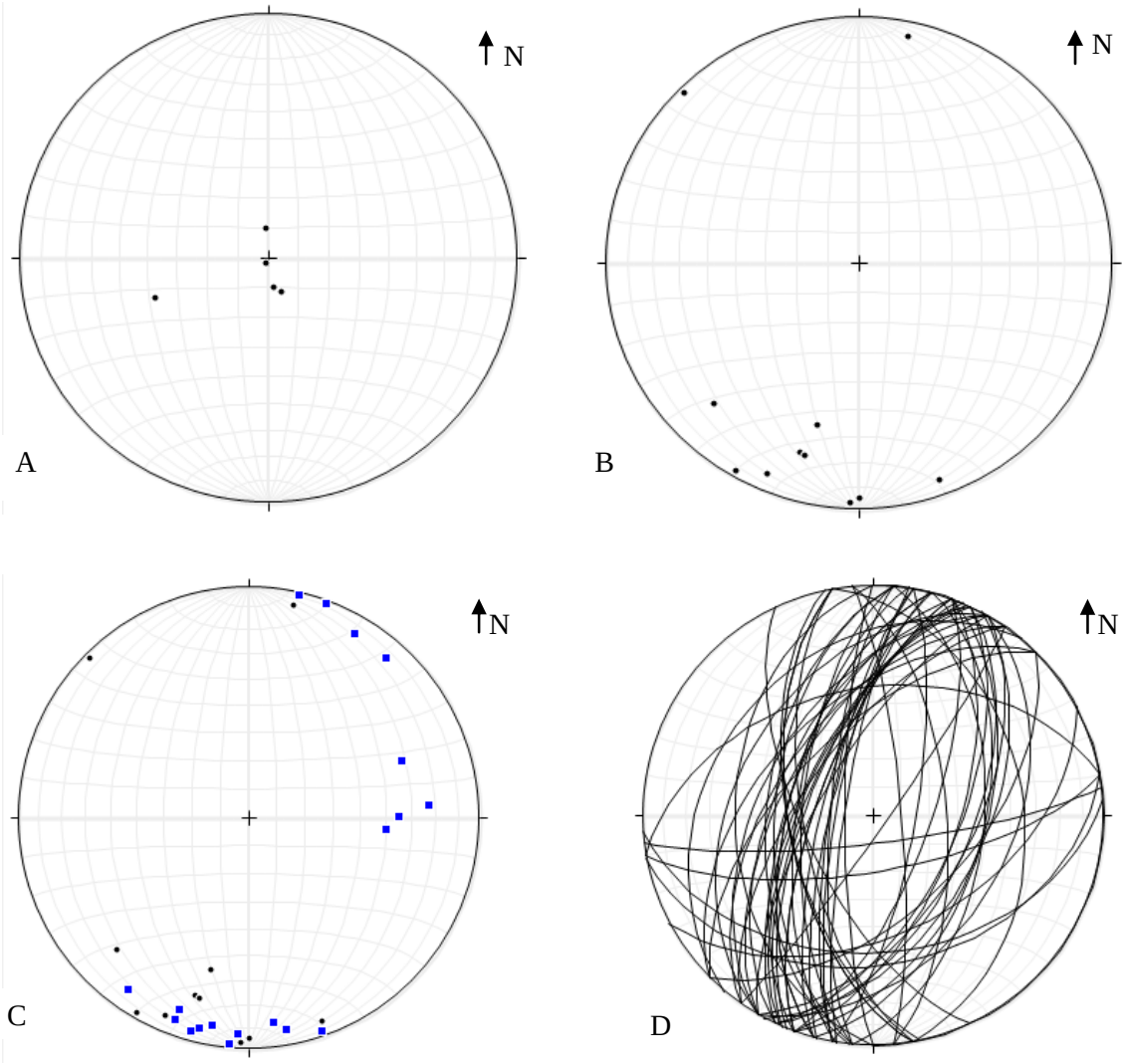


Figure 4.10 Lambert projection of geometric data A) Plots F1 folds with average plunging angle of $75^0$. *No. of Data: 5* B) Stereogram plots of F2 fold axis mostly concentrated on the south western region. It has an average attitude of ***$11.5^0 \rightarrow 189.4^0$.*** It coincides with the pole of π girdle drawn for the pole to foliation above. *No. of Data: 11* C) Plots of linear fabrics such as F2 fold axis (black circle), crenulation lineation and stretched pebbles dominantly plunging SSW at a shallow angle. No. of Data: 31 D) Planar data plots of foliation and bedding

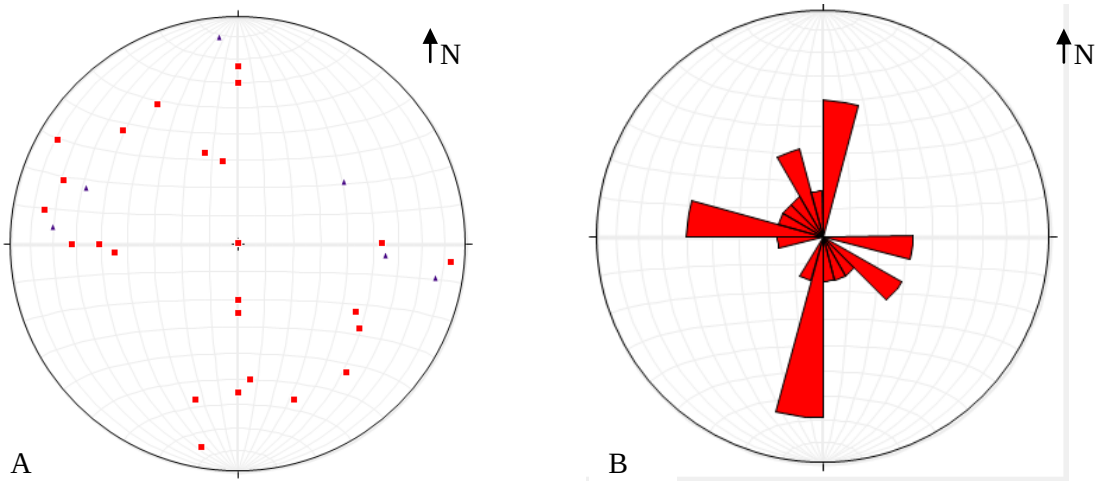


Figure 4.11 A) Plots of poles to joints and veins on lower hemisphere equal area net. Red box and blue triangle represents joints and veins respectively. B) Rose diagram of joints

# CHAPTER FIVE METAMORPHISM

## 5.1 INTRODUCTION

Metamorphism can be determined by careful analysis of the characteristics of the minerals constituting the rocks. Identifying how each and every mineral are affected by tectonic and related activities occurred throughout its formation is useful to evaluate the degree of metamorphism the rock has undergone. Analyzing to what extent the original structures and textures of the parent rocks are preserved in the rocks also helps us to understand the history of metamorphism. In addition, the characteristic minerals association and their degree of alteration in response to the pressure-temperature conditions they were subjected gives us important clue in dealing with metamorphism of the study area.

## 5.2 METAMORPHISM

The rocks of the study area have been subjected to different degree of deformation and metamorphism in which the original sedimentary and volcanic features are changed to varying extent. Some of the rocks have preserved the original relict minerals and primary textures and other show little mineralogical and textural changes.

In some of the rocks larger laths of plagioclase are being altered in to calcites with remnant albitic twinning left to identify the plagioclase. Chlorites and epidotes are formed as an alteration product of the mafic minerals during metamorphism.

In the metasediments, muscovite, sericite, and chlorites are characteristic assemblage of the low grade greenschist facies metamorphism along with quartz and plagioclase.

Low grade of metamorphism of the rocks of the study area can also be inferred from the presence of primary sedimentary structures such as bedding in metasediments (Fig 3.10B). Primary foliation (bedding) is also found in phyllite but it is not as prominent as it is on the slate and this is attributed to the increase in metamorphic grade in phyllites relative to the slate.

## 5.3 EFFECTS OF DEFORMATION ON METAMORPHISM

Analyzing the effect of deformation on individual metamorphic mineral grains is also useful to evaluate the conditions of metamorphism and related processes

Intra-crystalline deformations which are responsible for the formation of undulatory extinction in quartz (Fig 3.5A), feldspar and calcite are noticed in thin-sections. Irregular grain boundaries (Fig 3.5A, B, & 3.7 C) are also recognized that can be considered evidence for intra-crystalline deformation during dynamic recrystalization by grain boundary migration (Mantani et al., 2001; Passchier and Trouw 2005). Some of the quartz crystals show sub grains boundaries (3.5B & 3.7 C), a textural features pointing to recovery during dynamic recrystalization. The formation of elongate quartz ribbons (Fig 3.9A) are the results of the effects of low temperature in quartz minerals.

Core and mantle texture exist on some of the metavolcanic breccias (see Fig 3.7 D) is the result of deformation at low grade level which can further reveal the low grade metamorphism on the rocks of the study area. They are defined by larger quartz grains forming cores which are surrounded by smaller sub grains and dynamically recrystallized new grains around their margins.

## 5.4 MINERAL ASSEMBLAGES IN THE ROCKS OF THE STUDY AREA

The following are the most dominant mineral assemblages in the rocks of the study area including the critical minerals (underlined) useful to evaluate the grade of metamorphism.

1 Meta-basic

a . Chl +Ab + Ep + Qtz + Pl + Cal + Op.

2. Slate

a. Ser + Chl + Qtz + Op

b. Ser + Ms + Qtz + Op

c. Ser + Ms + Chl + Qtz + Pl + Op

d. Ser + Ms + Qtz + Pl + Op

3 Metavolcanic breccia

a. Chl + Qtz + Cal + Pl + Op.

b. Chl + Ms + Qtz + Cal + Op

4. Phylite

a. Ms + Ser + Qtz + Op.

5. Meta-dolomite

a. Dol + Cal+ Op

b. Dol + Cal+ Qtz+ Pl.

6. Meta-limestone

a. Cal + Qtz + Op

These mineral assemblages reveal that both metasedimantary and metavolcanic rocks of the study area have experienced metamorphism under a low grade greenschist facies.

Keys for abbreviations

Ser = Sericite Qtz = Quartz

Ab = Albite Pl = Plagioclase

Chl = Chlorite Op = Opaque

Ms = Muscovite

Cal = Calcite

## 5.5 TIME RELATION BETWEEN DEFORMATION AND METAMORPHISM

To relate the timing of the formation of minerals and deformation, it is important to examine closely the fabric alignments with respect to the porphyroblasts and porphyroclasts. When the porphyroblasts and porphyroclasts are wrapped by external fabrics (the main foliation), they are considered pre-tectonic (Fig 5.1A & C). Minerals such as sericite, muscovite, including elongate quartz ribbons are usually seen aligned parallel with the S1 foliation as a result of earlier deformation D1 (Fig 3.3B, 3.9A & 5.1 B). Thus they can be characterized as syn-D1 metamorphism. D2 deformation later came which folded S1 foliation to form second phase mineral assemblage. Mica minerals are observed axial planar to D2 fold axis to form M2 mineral assemblage (Fig 3.9A& 5.1B).

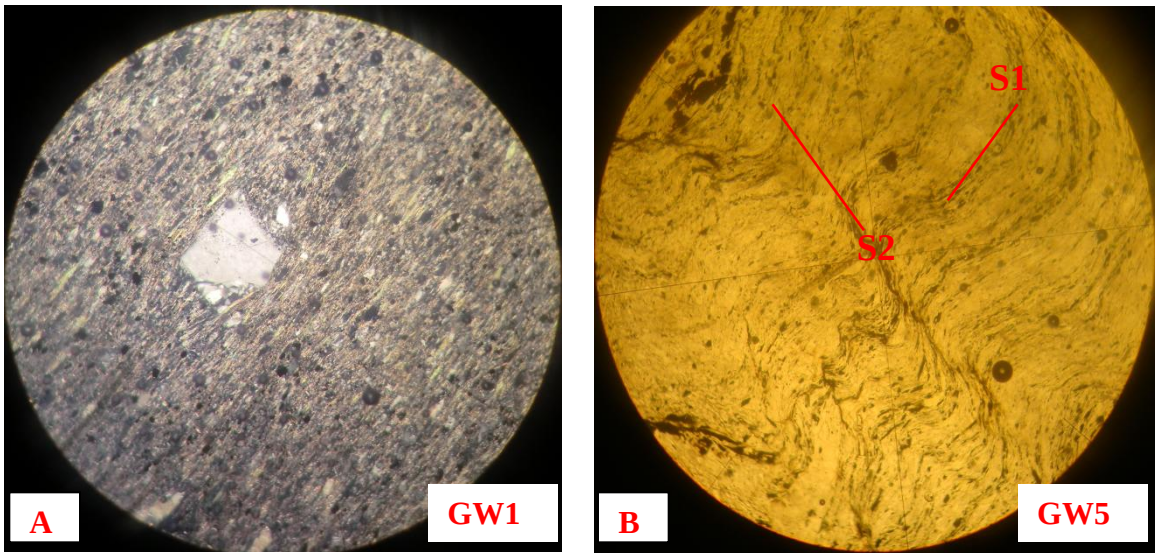

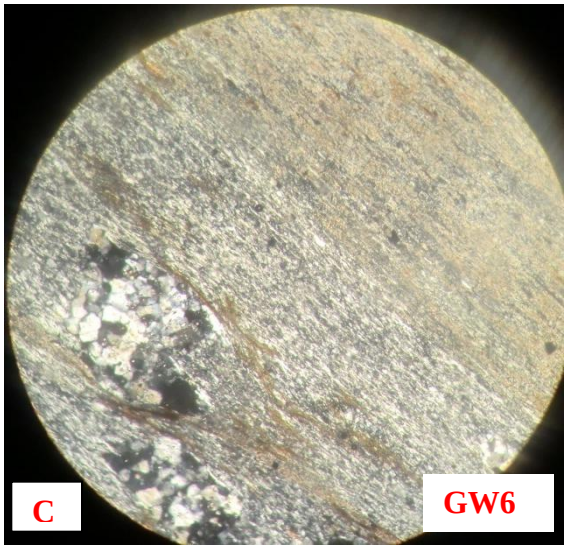


Figure 5.1 Photomicrographs of slate and phyllite A) Pre-tectonic porphyrobalst observed under XPL. Sample location 0568194E, 1552065N. B) S2 foliation on phyllite observed under PPL. Sample location; 0567923E, 1554242N C) Deflection of external foliation around pophyroclasts on the slate observed under XPL. Sample location; 0568063E, 1554265N. *Total magnification; 10x10=100x.*

# CHAPTER SIX CONCLUSION AND RECOMMENDATION

## 6.1 CONCLUSION

The study area is covered by metamorphic rocks of igneous and sedimentary origin which can tell us about the tectonic and metamorphic history of the area. The rocks include Meta-basic, Metavolcanic-brecias, Phyllite, Slate, Meta-dolomite and Meta-limestone. Some of these rocks maintained the original sedimentary bedding and other relict minerals.

Both metavolcanic and metasedimetary rocks have preserved evidences of the major tectonic activities occurred in the study area throughout the geologic history. They are low grade metamorphic rocks experiencing low pressure and temperature under a greenschist facies. The constituent low grade metamorphic minerals mostly of mica and quartz minerals and their fabric alignment in response to their respective deformation phases are used to characterize the metamorphic conditions.

The presence of superimposed folds and other associated structures indicate that the rocks are refolded by two phases of ductile deformation. Deformations phases are deduced which are responsible for the development of S1, and S2. The main regional foliation S1 have developed during M1 and D1 and are defined by mica minerals. Tight and isoclinal F1 folds are the other structural imprints of D1 phase. Compresional D2 stress which caused thickening of the crust due to the E-W directed horizontal shortening perpendicular to the stretching direction is followed by the formation folds of larger interlimb angle and horizontal axis, and also the re-alignment of fabrics to form M2 mineral assemblages oriented parallel with S2.

Two types of lineations are noticed on the study area. Generally N-S oriented lineations which are parallel to the prominent regional foliation and F2 fold axis and ENE-WNW directed elongation lineations nearly perpendicular to the regional fold axis. The first is L2 crenulation lineation associated with D2 and the second one is L1 lineation formed during D1 deformation.

## 6.2 RECOMMENDATION

- This study covers one limb of the Guwila syncline. Detailed studied on the syncline as a whole is needed to characterize the nature of its fold axis with the regional Negash syncline.
- Studies of isotope chemistry on the carbonate rocks of the study area is required to understand the paleo-environment of the area
- Some of the areas show intense veining of quartz and associated pyrite and other minerals. Thus there could be economic mineralization in the study area and studies focused on mineralization should be conducted.

## REFERENCES

Abdelsalam, M.G., and Stern, R.J., 1996. Sutures and shear zones in the Arabian-Nubian Shield. Journal of African Earth Sciences 23, 289-300.

Aguma, A., and Kebede, G. (1976) Geological map of Adi Ramet (ND37-9), 1: 250,000. Ethiopian Institute of Geological Survey, Ministry of Mines and Energy, Addis Ababa, Memoir No. 4

Alene M., Jenkin G., Leng M. and Darbyshir F. (2006). The Tambien Group, Ethiopia: an early Cryogenian (Ca. 800-735 Ma) Neoproterozoic sequence in the Arabian-Nubian Shield, Precambrian Research. **147**: 79-99.

Asrat, A., Barbey, P., and Gleizes, G. (2001). The Precambrian Geology of Ethiopia: a review, Africa Geoscience Review. **8**: 271-288.

Asrat, A., Gleizesc, G., Barbey, P., and Ayalew, D. (2003). Magma emplacement and mafic–felsic magma hybridization: structural evidence from the Pan-African Negash pluton, Northern Ethiopia. Journal of Structural Geology. 25: 1451-1469

Arkin, Y., Beyth, M., Dow, D.B., Levitte, B., Temesgen, H.,Tsegaye H., 1971. The Geological map of Mekele area (1:250,000). Ministry of Mines, Addis Ababa.

Avigad,D., Stern,R.J., Beyth, M., Miller, N., McWilliams, M.O.,2007. Detrital zircon U-Pb geochronology of Cryogenian diamictites and Lower Paleozoic sandstone in Ethiopia (Tigrai): Age constraints on Neoproterozoic glaciation and crustal evolution of the southern Arabian-Nubian Shield. Precambrian Research 154, 88-106.

Bailo, T., Schandelmeier, H., Franz, G., Chih-Hsien Sun., Stern, R.J. (2003). Plutonic and metamorphic rocks from the Keraf Suture (NE Sudan): a glimpse of Neoproterozoic tectonic evolution on the NE margin of W. Gondwana, Precambrian Research **123**: 67-80.

Beyth, M. (1971) The geology of central and western Tigre. Unpub.report, Ministry of Mines, Addis Ababa.

Beyth M. (1972). The geology of central and western Tigre. PhD Thesis, University of Bonn, Germany, 155pp.

Beyth, M., Avigad, D., Wetzel, H.U., Matthews, A., Berhe, S.M., 2003. Crustal exhumation and indications for Snowball Earth in the East African Orogen: North Ethiopia and East Eritrea. Precambrian Research **123**: 187–201.

Bingen, B., Jacobs, J., Viola, G., Henderson, I.H.C., Skår, Ø., Boyd, R., Thomas, R.J., Solli, A., Key, R.M., Daudi, E.X.F. (2009). Geochronology of the Precambrian crust in the Mozambique belt in NE Mozambique, and implications for Gondwana assembly, Precambrian Research **170**: 231-255.

Condie, K.C. (2003). Super continents, Superplumes and Continental growth: The Neoproterozoic Record, Department of Earth and Environmental Science, New Mexico Institute of Mining & Technology, Socorro, NM 87801.

Garland, C.R, 1972. Geological Map of Adigrat Area. 1:250,000 (ND 37-7). GSE, Addis Ababa,Ethiopia.

Garland C.R., (1980). Geology of the Adigrat Area. Ministry of Mines, Addis Ababa. Memoir No.1: 51.

Genna, A., Nehlig, P., Le Goff, E., Guerrot, C. & Shanti, M. (2002). Proterozoic tectonism of the Arabian Shield, Precambrian Research. **117**: 21-40

Johnson P. and Beraki Weldehaimanot, (2003). Development of the Arabian-Nubian Shield: perspectives on accretion and deformation in the northern East African Orogen and the assembly of Gondwana, Geological Society, London. p289-325.

Kazmin V., (1972). The geology of Ethiopia. Ethiopian Institute of Geological Surveys. Note No. 821-051-12: 208.

Kazmin, V. (1973). The geological map of Ethiopia, 1:2,000,000. Ethiopian Institute of Geological Surveys, Addis Ababa, Ethiopia.

Kazmin, V., Shiferaw, A., Balcha, T., 1978. The Ethiopian basement: stratigraphy and possible manner of evolution. Geologische Rundschau 67, 531–548.

Kroner, A., and Stern, R.J., 2005. AFRICA/Pan- African Orogeny. Encyclopedia of Geology, v. 1. Elsevier, Amsterdam

Levitte D., (1970). The geology of central part of Mekelle sheet (ND37-11). Ethiopian Institute of Geological Survey. Note No. 821-201-12: 66.

Mantani, A., Merh, S.S., Karanth, R.V., Greiling, R.O. (2001) Time relationship between metamorphism and deformation in Proterozoic rocks of the Lunavada region, Southern Aravalli Mountain Belt (India) - a microstructural study, Journal of Asian Earth Science**19**: 195-205.

Miller, N.R., Alene, M., Sacchi, R., Stern, R.J., , Conti, A., Kröner, A., Zuppi, G .,2003. Significance of the Tambien Group (Tigrai, N. Ethiopia) for Snowball Earth events in the Arabian–Nubian Shield. Precambrian Research 121 (2003) 263–283.

Miller, N.R., Avigad, D., Stern, R.J., Beyth, M. & Schilman, B. (2009) Cryogenian slate carbonate sequences of the Tambien Group, Northern Ethiopia (I): Pre-"Sturtian" chemostratigraphy and regional correlations, Precambrian Research **170**: 129–156.

Miller, N.R., Avigad, D., Stern, R.J. and Beyth, M. (2011).The Tambien Group, Northern Ethiopia (Tigre), Geological Society of London. **36**: 263-276.

Mogessie, A., Krenn, K., Schaflechner, K., Koch, J.U., Egger, T., Goritching, B., Kesednar, B., Pichler, H., Ofner, L., Bauernfeind, D., Tadesse, S. and Demessie, M. (2002). A Geological Excursion to the Mesozoic Sediments of the Abay Bain (Blue Nile): Recent Volcanics of the Ethiopian Main Rift and Basement Rocks of the Adola Area, Ethiopia, Mitt.Osterr.Miner.Ges. 147.

Passchier.C. and Trouw.R.J.(2005). Microtectonics. Springer-Verlag Berlin Heidelberg, Germany.

Ramsay, J.G. (1967). Folding and Fracturing, The Black Burn Press. pp. 9

Sifeta, K., Roser, P., Kimura, J. (2005) Geochemistry, provenance, and tectonic setting of Neoproterozoic metavolcanic and metasedimentary units, Werri area, Northern Ethiopia, Journal of African Earth Science **41**: 212-234

Stern, R.J. (1994). Arc assembly and continental collision in the Neoproterozoic East African Orogen: implications for consolidation of Gondwana land, Annual Reviews Earth Planetary Sciences. **22**: 319-351.

Stern, R.J., 2002.Crustal evolution in the East African Orogen: a neodymium isotopic perspective. Journal of African Earth Sciences 34, 109–117.

Tadesse, G, and Allien, A. (2005). Geology and geochemistry of the Neoproterozoic Tuludimtu Ophiolite suite, western Ethiopia, Journal of African Earth Sciences **41**: 192–211.

Tadesse, T., 1996. Structure across a possible intra-oceanic suture zone in low-grade Pan-African rocks of northern Ethiopia. Journal of African Earth Sciences 23, 575-381.

Tadesse, T. (1997). Geology of Axum area. Ethiopian Institute of Geological Surveys, Addis Ababa. Memoir No.9: 187pp.

Tadesse, T., Hoshino, M., Sawada, Y. (1999). Geochemistry of low grade metavolcanic rocks from the Pan-African of the Axum area, northern Ethiopia, Precambrian Research. **99**: 101–124.

Tadesse, S., Milesi, J., Deschamps, Y. (2003). Geology and mineral potential of Ethiopia: a note on geology and mineral map of Ethiopia, Journal of African Earth Science. **39:** 273-313

Tefera, M., Chernet, T. and Haro, W. (1996). Explanation of the geological map of Ethiopia (scale 1:2,000,000), 2nd ed., Ethiopian institute of geological surveys. Addis Ababa, bulletin no. 3.

Warden, A.J., and Horkel, A.D. (1984). The Geological evolution of the NE-Branch of the Mozambique Belt (Kenya, Somalia, Ethiopia), Mitteilungen der Österr, Geol. Ges., Bd.77.

Worku, H. and Schandelmeier, H. (1996). Tectonic evolution of the Neoproterozoic Adola Belt of southern Ethiopia: evidence for a Wilson cycle process and implications for oblique plate collision, Precambrian Research. 77: 179–210.

Yibas, B., Reimond, W.U., Armstrong, R., Koeberl, C., Anhaeusser, C.R. and Phillips, D. (2002). The tectonostratigraphy, granitoid geochronology and geological evolution of the Precambrian of southern Ethiopia, Journal of African Earth Sciences. **34:** 57–84.

Yihunie, T. and Hailu, F. (2007). Possible eastward tectonic transport and northward gravitational tectonic collapse in the Arabian–Nubian shield of western Ethiopia, Journal of African Earth Sciences **49**: 1–11

# APPENDIX

Appendix-1 Structural measurements of different structural elements

| No | Measured structural element | Dip | Dip direction | Location | Unit |
|---|---|---|---|---|---|
| 1 | S1 | 40 | 090 | 0566489E, 1552784N | Metabasic |
| 2 | S1 | 60 | 260 | 0566948E 1552503N | Metabasic |
| 3 | S1 | 55 | 275 | 0567197E 1552102N | Slate |
| 4 | S0 | 80 | 173 | 0567420E 1552126N | Slate |
| 5 | S0 | 65 | 260 | 0567522E 1552265N | Slate |
| 6 | S1 | 50 | 095 | 0567874E 1552123N | Dolomite-slate intercalation |
| 7 | S1 | 70 | 290 | 0568072E 1552139N | Slate |
| 8 | S1 | 60 | 290 | 0568194E 1552065N | Slate |
| 9 | S1 | 75 | 100 | 0568285E 1552050N | Slate |
| 10 | S1 | 60 | 115 | 0568888E 1551958N | Slate |
| 11 | S0 | 60 | 285 | 0569096E 1551988N | Grey slate |
| 12 | S1 | 70 | 272 | 0569492E 1551839N | Dolomite-slate intercalation |
| 13 | S1 | 80 | 279 | 0570355E 1551809N | Dolomite-slate intercalation |
| 14 | S1 | 80 | 090 | 0570828E 1551963N | Limestone |
| 15 | S1 | 44 | 350 | 0571115E 1551809N | Limestone |
| 16 | S1 | 85 | 125 | 0568085E 1551821N | Grey slate |
| 17 | S1 | 75 | 275 | 0564324E 1548901N | Slate |
| 18 | S1 | 60 | 285 | 0565457E 1548415N | Slate |
| 19 | S1 | 65 | 275 | 0567172E 1548100N | Dolomite-Slate intercalation |
| 20 | S1 | 35 | 080 | 0567206E 1548192N | Dolomite-Slate intercalation |
| 21 | S0 | 80 | 085 | 0567679E 1548912N | Slate |
| 22 | S0 | 60 | 315 | 0567962E 1549054N | Slate |

| | | | | | |
|---|---|---|---|---|---|
| 23 | S1 | 70 | 170 | 0568319E 1549087N | Slate |
| 24 | S1 | 63 | 279 | 0568435E 1549320N | Dolomite-slate intercalation |
| 25 | S1 | 50 | 110 | 0569923E 1549102N | Dolimite-slate intercalation |
| 26 | S0 | 50 | 300 | 0570347E 1548736N | Limestone |
| 27 | S1 | 67 | 292 | 0567628E 1554143N | Slate |
| 28 | S1 | 75 | 284 | 0567923E 1554242N | Phyllite |
| 29 | S1 | 75 | 280 | 0567983E 1554368N | Phyllite |
| 30 | S1 | 40 | 120 | 0568063E 1554265N | Slate |
| 31 | S0 | 71 | 300 | 0568653E 1554382N | Slate |
| 32 | S1 | 65 | 305 | 0568917E 1554384N | Grey slate |
| 33 | S1 | 64 | 295 | 0569424/1554268 | Slate |
| 34 | S1 | 30 | 310 | 0569714E 1554193N | Dolomite-slate intercalation |
| 35 | S1 | 55 | 135 | 0570220E 1553820N | Dolomite-slate intercalation |
| 36 | S1 | 60 | 110 | 0570592E 1553877N | Dolomite-slate intercalation |
| 37 | S0 | 50 | 315 | 0571012E 1553879N | Limestone |
| 38 | S0 | 55 | 120 | 0571086E 1553840N | Limestone |
| 39 | S1 | 77 | 280 | 0566708E 1552215N | Metavolcanic breccia |
| 40 | S1 | 72 | 285 | 0567134E 1551897N | Metavolcanic breccia |
| 41 | S1 | 70 | 290 | 567301 E 1551780N | Slate |
| 42 | S1 | 50 | 105 | 0567421E 1550904N | Dolomite-slate intercalation |
| 43 | S1 | 55 | 115 | 0567906E 1551780N | Slate |
| 44 | S1 | 55 | 115 | 0568500E 1551199N | Slate |
| 45 | S1 | 60 | 260 | 0568578E 1551097N | Grey slate |
| 46 | S0 | 40 | 300 | 0570627E 1550392N | Limestone |
| 47 | S1 | 65 | 294 | 0567114E 1551843N | Metavolcanic breccia |
| 48 | S1 | 58 | 300 | 0566563E 1550787N | Metabasic |

| | | | | | |
|---|---|---|---|---|---|
| 49 | S1 | 55 | 125 | 0567686E 1552743N | Metavolcanic breccia |
| 50 | S0 | 50 | 118 | 0570860E 1549151N | Limestone |
| 51 | S1 | 65 | 080 | 0568850E 1549220N | Dolomite-slate intercalation |
| 52 | S1 | 47 | 152 | 0566309E 1547772N | Slate |
| 53 | S0 | 60 | 258 | 0568501E 1550188N | Slate |
| 54 | S1 | 40 | 176 | 0566680E 1552801N | Metabasic |
| 55 | S1 | 64 | 095 | 0568720E 1553510N | Grey slate |
| 56 | S1 | 35 | 169 | 0569902E 1553830N | Grey slate |
| 57 | S1 | 65 | 245 | 05679312/1554102 | Metavolcanic breccia |
| 58 | S1 | 52 | 097 | 0570643E1550823N | Limestone |
| 59 | S1 | 40 | 300 | 0570478E 1550981N | Dolomite-slate intercalation |
| No. | Measured structural element | dip | Dip direction | Location | Unit |
| 1 | Joints | 25 | 090 | 0566584E, 1552583N | Slate |
| 2 | Joints | 60 | 090 | 0566738E 1553506N | Metabasic |
| 3 | Joints | 20 | 090 | 0568297E 1552542N | Grey slate |
| 4 | Joints | 80 | 120 | 0569410E 1554127N | Slate |
| 5 | Joints | 62 | 340 | 0567522E 1552265N | Dolomite-slate intercalation |
| 6 | Joints | 90 | 090 | 0566774E 1553223N | Metabasic |
| 7 | Joints | 65 | 000 | 0567162E 1552159N | Slate |
| 8 | Joints | 70 | 110 | 0568293E 1551085N | Dolomite-slate |
| 9 | Joints | 30 | 170 | 0568396E 1552150N | slate |
| 10 | Joints | 35 | 160 | 0569428E 1551658N | Slate |
| 11 | Joints | 63 | 140 | 0569096E 1551988N | Grey slate |
| 12 | Joints | 55 | 270 | 0566484E 1553363N | Metabasic |
| 13 | Joints | 60 | 135 | 0567252E 1552458N | Slate |

| | | | | | |
|---|---|---|---|---|---|
| 14 | Joints | 50 | 355 | 0570193E 1552385N | Dolomite-slate |
| 15 | Joints | 83 | 275 | 0569596E 1554152N | Dolomite-slate |
| 16 | Joints | 75 | 100 | 0569217E 1551456N | Dolomite-slate |
| 17 | Joints | 51 | 000 | 0569105E 1550838N | Dolomite-slate |
| 18 | Joints | 45 | 084 | 0567395E 1551153N | Dolomite-slate |
| 19 | Joints | 53 | 000 | 0566528E 1552648N | Slate |
| 20 | Joints | 60 | 150 | 0569695E 1551783N | Dolomite-slate |
| 21 | Joints | 67 | 090 | 0570347E 1548736N | Limestone |
| 22 | Joints | 80 | 190 | 0567628E 1554143N | Slate |
| 23 | Joints | 60 | 195 | 0567923E 1554242N | Phyllite |
| No. | Fold axis | Plunge | Plunge direction | Location | Unit |
| 1 | F1 | 80 | 355 | 0569695E 1551783N | Dolomite-slate |
| 2 | F1 | 88 | 204 | 0567395E 1551153N | Dolomite-slate |
| 3 | F1 | 78 | 160 | 0570478E 1550981N | Dolomite-slate |
| 4 | F1 | 50 | 250 | 0567301E 1551780N | Dolomite-slate |
| 5 | F1 | 80 | 170 | 0570478E 1550981N | Dolomite-slate |
| 6 | F2 | 07 | 160 | 0567679E 1548912N | Slate |
| 7 | F2 | 21 | 197 | 0567987E 1549161N | Slate |
| 8 | F2 | 07 | 012 | 0568334E 1549197N | Slate |
| 9 | F2 | 03 | 210 | 0568334E 1549197N | Slate |
| 10 | F2 | 03 | 182 | 0570950E 1549253N | Limestone |
| 1 | F2 | 03 | 315 | 0570368E 1550781N | Dolomite-slate intercalation |
| 12 | F2 | 05 | 180 | 0568072E 1552139N | Slate |
| 13 | F2 | 08 | 203 | 0568194E 1552065N | Slate |
| No. | Axial plane | Dip | Dip direction | Location | Unit |

| | | | | | |
|---|---|---|---|---|---|
| 1 | Axial plane | 10 | 090 | 0566948E 1552503N | Slate |
| 2 | Axial plane | 71 | 102 | 0567197E 1552102N | Slate |
| 3 | Axial plane | 5 | 082 | 0568063E 1554265N | Slate |
| 4 | Axial plane | 70 | 205 | 0567987E 1549161N | Slate |
| 5 | Axial plane | 70 | 188 | 0568334E 1549197N | Slate |
| 6 | Axial plane | 60 | 157 | 0569613E 1554194N | Dolomite-slate intercalation |
| 7 | Axial plane | 83 | 017 | 0570121E 1553720N | Dolomite-slate intercalation |
| 8 | Axial plane | 10 | 000 | 0568450E 1551231N | slate |
| 9 | Axial plane | 05 | 017 | 0568500E 1551199N | slate |
| 10 | Axial plane | 71 | 347 | 0570482E 1553907N | Dolomite slate intercalation |
| 11 | Axial plane | 70 | 330 | 0568850E 1549220N | Dolomite-slate intercalation |
| 12 | Axial plane | 65 | 140 | 0568160E 1548974N | Dolomite-slate intercalation |
| No. | Lineation | Plunge | Plunge direction | Location | Unit |
| 1 | Crenulation lineation | 5 | 195 | 0566708E 1552215N | Metavolcanic breccia |
| 2 | Crenulation lineation | 10 | 041 | 0566708E 1552215N | Metavolcanic breccia |
| 3 | Crenulation lineation | 02 | 013 | 0567631E 1553292N | Phllite |
| 4 | Crenulation lineation | 07 | 183 | 0567709E 1553602 | Phllite |
| 5 | Crenulation lineation | 10 | 190 | 0567808E 1553868N | Phllite |
| 6 | Crenulation lineation | 08 | 170 | 0567133E 1552163N | Metavolcanic breccia |
| 7 | Crenulation lineation | 10 | 030 | 0566989E 1551598N | Metavolcanic breccia |
| 8 | Crenulation lineation | 12 | 173 | 0566843E 1551133N | Metavolcanic breccia |
| 9 | Crenulation lineation | 08 | 200 | 0567177E 1552174N | Metavolcanic breccia |
| 10 | Crenulation lineation | 193 | 007 | 0567122E 1551200N | Phllite |
| 11 | Crenulation lineation | 161 | 003 | 0567277E 1552727N | Metavolcanic breccia |
| 12 | Crenulation lineation | 200 | 013 | 0567310E 1551919N | Phllite |
| 13 | Crenulation | 215 | 010 | 0567454E 1552439N | Phllite |

| | | | | | |
|---|---|---|---|---|---|
| | lineation | | | | |
| 14 | Crenulation lineation | 231 | 006 | 0567089E 1551963N | Metavolcanic breccia |
| 15 | Stretching lineation | 40 | 095 | 0567114E, 1551843N | Metavolcanic breccia |
| 16 | Stretching lineation | 23 | 086 | 0567114E, 1551843N | Metavolcanic breccia |
| 17 | Stretching lineation | 30 | 070 | 0567125E, 1551835N | Metavolcanic breccia |
| 18 | Stretching lineation | 35 | 090 | 0567119E, 1551853N | Metavolcanic breccia |

## DECLARATION OF ORIGINALITY

This thesis is my original work and has not been presented for a degree in any other university, and that all sources of material used for the thesis have been duly acknowledged.

…….. ….……

Desta Dawit (Candidate) Date

This is to certify that the above declaration made by the candidate is correct to the best of my knowledge.

…….. …….

Dr. Mulugeta Alene (Advisor) Date